Probability distributions of linear statistics in chaotic cavities and associated phase transitions

Pierpaolo Vivo

Abdus Salam International Centre for Theoretical Physics, Strada Costiera 11, 34151 Trieste, Italy

Satya N. Majumdar and Oriol Bohigas

Laboratoire de Physique Théorique et Modèles Statistiques, UMR 8626 du CNRS,
Université Paris-Sud, Bâtiment 100, 91405 Orsay Cedex, France

We establish large deviation formulas for linear statistics on the N transmission eigenvalues $\{T_i\}$ of a chaotic cavity, in the framework of random matrix theory. Given any linear statistics of interest $A = \Sigma_{i=1}^{N} a(T_i)$, the probability distribution $\mathcal{P}_A(A, N)$ of A generically satisfies the large deviation formula $\lim_{N \to \infty} [-2 \log \mathcal{P}_A(Nx, N)/\beta N^2] = \Psi_A(x)$, where $\Psi_A(x)$ is a rate function that we compute explicitly in many cases (conductance, shot noise, and moments) and β corresponds to different symmetry classes. Using these large deviation expressions, it is possible to recover easily known results and to produce new formulas, such as a closed form expression for $v(n) = \lim_{N \to \infty} \text{var}(\mathcal{T}_n)$ (where $\mathcal{T}_n = \Sigma_i T_i^n$) for arbitrary integer n. The universal limit $v^* = \lim_{n \to \infty} v(n) = 1/2\pi\beta$ is also computed exactly. The distributions display a central Gaussian region flanked on both sides by non-Gaussian tails. At the junction of the two regimes, weakly nonanalytical points appear, a direct consequence of phase transitions in an associated Coulomb gas problem. Numerical checks are also provided, which are in full agreement with our asymptotic results in both real and Laplace space even for moderately small N. Part of the results have been announced by Vivo *et al.* [Phys. Rev. Lett. **101**, 216809 (2008)].

I. INTRODUCTION

We consider the statistics of quantum transport through a chaotic cavity with $N_1 = N_2 = N \gg 1$ open channels in the two attached leads. It is well established that the electrical current flowing through a cavity of submicron dimensions presents time-dependent fluctuations which persist down to zero temperature[1] and are thus associated with the granularity of the electron charge e. Among the characteristic features observed in experiments, we can mention weak localization,[2] universality in conductance fluctuations,[3] and constant Fano factor.[4] In the Landauer-Büttiker scattering approach,[1,5,6] the wave-function coefficients of the incoming and outgoing electrons are related through the unitary scattering matrix $S(2N \times 2N)$

$$S = \begin{pmatrix} r & t' \\ t & r' \end{pmatrix}, \tag{1}$$

where the transmission (t, t') and reflection (r, r') blocks are $(N \times N)$ matrices encoding the transmission and reflection coefficients among different channels. Many quantities of interest for the experiments can be extracted from the eigenvalues of the hermitian matrix $tt^\dagger$: for example, the dimensionless conductance and the shot noise are given, respectively, by $G = \text{Tr}(tt^\dagger)$ (Ref. 5) and $P = \text{Tr}[tt^\dagger(1 - tt^\dagger)]$.[7,8]

Random matrix theory has been very successful in describing the statistics of universal fluctuations in such systems and complements the fruitful semiclassical approach.[9–13] The simplest way to model the scattering matrix S for the case of chaotic dynamics is to assume that it is drawn from a suitable ensemble of random matrices with the overall constraint of unitarity.[14–17] Through a maximum entropy approach with the assumption of ballistic point

contacts,[1] one derives that the probability distribution of S should be uniform within the unitary group, i.e., S belongs to one of Dyson's circular ensembles.[18,19]

It is then a nontrivial task to extract from this information the joint probability density (jpd) of the transmission eigenvalues $\{T_i\}$ of the matrix $tt^\dagger$, from which the statistics of interesting experimental quantities could be, in principle, derived. Fortunately, this can be done[1,16,20,21] and the expression reads

$$P(T_1, \ldots, T_N) = A_N \prod_{j<k} |T_j - T_k|^\beta \prod_{i=1}^{N} T_i^{\beta/2-1}, \tag{2}$$

where the Dyson index β characterizes different symmetry classes ($\beta = 1, 2$ according to the presence or absence of time-reversal symmetry and $\beta = 4$ in case of spin-flip symmetry). The eigenvalues T_i are correlated random variables between 0 and 1. The constant A_N is explicitly known from the celebrated Selberg's integral as

$$A_N^{-1} = \prod_{j=0}^{N-1} \frac{\Gamma\left(1 + \frac{\beta}{2} + j\frac{\beta}{2}\right) \Gamma\left[\frac{\beta}{2}(j+1)\right] \Gamma\left(1 + j\frac{\beta}{2}\right)}{\Gamma\left(1 + \frac{\beta}{2}\right) \Gamma\left[\frac{\beta}{2} + 1 + (N + j - 1)\frac{\beta}{2}\right]}. \tag{3}$$

From Eq. (2), in principle, the statistics of all observables of interest can be calculated. In this paper, we shall focus on the following:

$$G = \sum_{i=1}^{N} T_i \quad \text{(conductance)}, \tag{4}$$

$$P = \sum_{i=1}^{N} T_i(1 - T_i) \quad \text{(shot noise)}, \tag{5}$$

$$\mathcal{T}_n = \sum_{i=1}^{N} T_i^n \quad \text{(integer moments)} \tag{6}$$

although, in principle, any linear statistics[22] $A = \sum_{i=1}^{N} a(T_i)$ can be tackled with the method described below. It is worth mentioning that an increasing interest for the moments and cumulants of the transmission eigenvalues can be observed in recent theoretical[23] and experimental works.[24]

Many results are known for the average and the variance of the above quantities, both for large N (Refs. [1], [25], and [26]) and, very recently, also for a fixed and finite number of channels N_1, N_2.[26–29] In particular, a general formula for the variance of any linear statistics $A = \sum_{i=1}^{N} a(\lambda_i)$ [where $T_i = (1 + \lambda_i)^{-1}$] in the limit of large number of open channels is known from Beenakker.[30] However, at least for the case $A = \mathcal{T}_n$ (integer moments), this formula is of little practical use. The method we introduce below allows to obtain the sought quantity $v(n) = \lim_{N \to \infty} \text{var}(\mathcal{T}_n)$ in a neat and explicit way.

In contrast with the case of mean and variance, for which a wealth of results are available (see, e.g., Refs. [1] and [31], and references therein), much less is known for the *full* distribution of the quantities above: for the conductance, an explicit expression was obtained for $N_1 = N_2 = 1, 2$ (Refs. [32–34]) while more results are available in the case of quasi-one-dimensional wires[35] and three-dimensional insulators.[36] For the shot noise, the distribution was known only for $N_1 = N_2 = 1$.[37] Very recently, Sommers *et al.*[38] announced two formulas for the distribution of the conductance and the shot noise, valid at arbitrary number of open channels and for any β, which are based on Fourier expansions. Such results are then incorporated and expanded in Ref. [39]. In Refs. [40] and [41] along with recursion formulas for the efficient computation of conductance and shot noise cumulants, an asymptotic analysis for the distribution functions of these quantities in the limit of many open channels was reported. In a recent letter,[42] we announced the computation of the same asymptotics (in the form of large deviation expressions) using a Coulomb gas method and we pointed out a significant discrepancy with respect to the claims by Osipov and Kanzieper.[40,41] We will discuss in detail this disagreement and the way to sort it out convincingly in Sec. IV D for the conductance case for $\beta = 2$.

The results of Refs. [38] and [39] concerning the distribution of conductance are formal in nature in the form of an $(N \times N)$ determinant and it is difficult to obtain an explicit form for the distribution in the large N limit. The advantage of the Coulomb gas approach, used in this paper, is that it provides an explicit expression for the full distribution of the conductance and shot noise in the large N limit. Given some recent experimental progresses,[43] which made eventually possible to explore the full distribution for the conductance (and not just its mean and variance), it is of great interest to deepen our knowledge about distributions of other quantities, whose experimental test may be soon within reach.
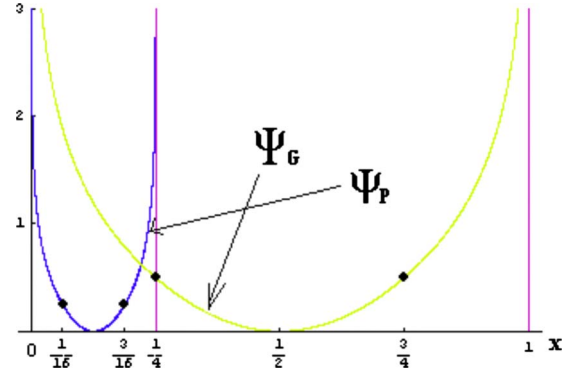

FIG. 1. (Color online) $\Psi_G(x)$ and $\Psi_P(x)$ as in Eqs. (8) and (10). The black dots highlight the critical points on each curve.

It is the purpose of the present paper to build on[42] and establish exact large deviation formulas for the distribution of any linear statistics on the transmission eigenvalues of a symmetric cavity with $N_1 = N_2 = N \gg 1$ open channels. More precisely, for any linear statistics A whose probability density function (pdf) is denoted as $\mathcal{P}_A(A, N)$, we have[44]

$$\lim_{N \to \infty} \left[-\frac{2 \log \mathcal{P}_A(A = Nx, N)}{\beta N^2} \right] = \Psi_A(x), \tag{7}$$

where the large deviation function $\Psi_A(x)$ (usually called *rate function*) is computed exactly for conductance $(A = G)$, shot noise $(A = P)$, and integer moments $(A = \mathcal{T}_n)$. The method can be extended to the case of asymmetric cavities $N_1 = \kappa N_2$ and is based on a combination of the standard Coulomb gas analogy by Dyson and functional methods recently exploited in Ref. [45] in the context of Gaussian random matrices. This approach has been then fruitfully applied to many other problems in statistical physics.[45–53]

The paper is organized as follows. Section II provides a quick summary of our main results. In Sec. III, we summarize the Coulomb gas method that can, in principle, be used to obtain the rate function associated with arbitrary linear statistics. In Secs. IV–VI, we use this general method to obtain explicit results, respectively, for the conductance, shot noise, and integer moments. Finally we conclude in Sec. VII with a summary and some open problems.

II. SUMMARY OF RESULTS

A. Distribution of conductance G

We obtain the following exact expression for the rate function in the case of conductance (G) (Fig. 1):

$$\Psi_G(x) = \begin{cases} \dfrac{1}{2} - \log(4x) & \text{for } 0 \leq x \leq \dfrac{1}{4} \\[2mm] 8\left(x - \dfrac{1}{2}\right)^2 & \text{for } \dfrac{1}{4} \leq x \leq \dfrac{3}{4} \\[2mm] \dfrac{1}{2} - \log[4(1 - x)] & \text{for } \dfrac{3}{4} \leq x \leq 1 \end{cases}. \tag{8}$$

The rate function has a quadratic form near its minimum at $x = 1/2$ in the range $1/4 \leq x \leq 3/4$. Using Eq. (7), it then

follows that the distribution $\mathcal{P}_G(G,N)$ has a Gaussian form close to its peak

$$\mathcal{P}_G(G,N) \approx \exp\left[-\frac{\beta}{2}N^2\Psi_G\left(\frac{G}{N}\right)\right]$$

$$= \exp\left[-\frac{\beta}{2}N^2 8\left(\frac{G}{N}-\frac{1}{2}\right)^2\right]$$

$$= \exp\left[-\frac{1}{2(1/8\beta)}\left(G-\frac{N}{2}\right)^2\right] \qquad (9)$$

from which one easily reads off the mean and variance $\langle G\rangle = N/2$ and $\text{var}(G) = 1/8\beta$, which agree with their known large N values. The fact that the variance becomes independent of N for large N is referred to as the *universal conductance fluctuations*. This central Gaussian regime is valid over the region $N/4 \le G \le 3N/4$. Outside this central zone, $\mathcal{P}_G(G,N)$ has non-Gaussian large deviation power-law tails. Using Eq. (8) in Eq. (7) near $x=0$ and $x=1$, we get $\mathcal{P}_G(G,N) \sim G^{\beta N^2/2}$ (as $G\to 0$) and $\mathcal{P}_G(G,N) \sim (N-G)^{\beta N^2/2}$ (as $G\to N$) which are in agreement, to leading order in large N, with the exact far tails obtained in Refs. 38, 39, and 54. It turns out that while the central Gaussian regime matches continuously with the two side regimes, there is a weak singularity at the two critical points $G=N/4$ and $G=3N/4$ (only the third derivative is discontinuous). One of our central results is to show that these two weak singularities in the conductance distribution arise due to two phase transitions in the associated Coulomb gas problem where the average charge density undergoes abrupt changes at these critical points. We note that an intermediate regime with an exponential tail claimed in Refs. 40 and 41 does not appear in our solutions, and we will comment in detail about such discrepancy in Sec. IV D.

B. Distribution of shot noise P

For the shot noise, the exact rate function reads

$$\Psi_P(x) = \begin{cases} \dfrac{1}{4} - 2\log 2 - \dfrac{1}{2}\log x & \text{for } 0\le x\le \dfrac{1}{16} \\[2mm] 64\left(x-\dfrac{1}{8}\right)^2 & \text{for } \dfrac{1}{16}\le x\le \dfrac{3}{16} \\[2mm] \dfrac{1}{4} - 2\log 2 - \dfrac{1}{2}\log\left(\dfrac{1}{4}-x\right) & \text{for } \dfrac{3}{16}\le x\le\dfrac{1}{4} \end{cases}.$$
$$(10)$$

Thus the shot noise distribution $\mathcal{P}_P(P,N)$, in the large N limit, also has a central Gaussian regime over $N/16\le P \le 3N/16$ where

$$\mathcal{P}_P(P,N) \approx \exp\left[-\frac{\beta}{2}N^2\Psi_P\left(\frac{P}{N}\right)\right]$$

$$= \exp\left[-\frac{\beta}{2}N^2 64\left(\frac{P}{N}-\frac{1}{8}\right)^2\right]$$

$$= \exp\left[-\frac{1}{2(1/64\beta)}\left(P-\frac{N}{8}\right)^2\right] \qquad (11)$$

yielding $\langle P\rangle = N/8$ and $\text{var}(P)=1/64\beta$. As in the case of conductance, this central Gaussian regime is flanked on both sides by two non-Gaussian power-law tails with weak third-order singularities at the transition points $P=N/16$ and $P=3N/16$.

C. Distribution of integer moments $\mathcal{T}_n$

For general $n>1$, the computation of the full rate function $\Psi_{\mathcal{T}_n}(x)$ and hence the large N behavior of the distribution $\mathcal{P}_{\mathcal{T}_n}(\mathcal{T}_n,N)$ turns out to be rather cumbersome. However, the distribution $\mathcal{P}_{\mathcal{T}_n}(\mathcal{T}_n,N)$ shares some common qualitative features with the conductance and the shot-noise distributions. For example, we show that for any $n>1$, there is a central Gaussian regime where the rate function $\Psi_{\mathcal{T}_n}(x)$ has a quadratic form given exactly by

$$\Psi_{\mathcal{T}_n}(x) = \frac{b_n}{2}\left[x - \frac{\Gamma(n+1/2)}{\sqrt{\pi}\Gamma(n+1)}\right]^2, \qquad (12)$$

where $b_n = \frac{4\pi\Gamma(n)\Gamma(n+1)}{[\Gamma(n+1/2)]^2}$. This implies a Gaussian peak in the distribution

$$\mathcal{P}_{\mathcal{T}_n}(\mathcal{T}_n,N) \approx \exp\left\{-\frac{\beta}{2}N^2\frac{b_n}{2}\left[\frac{\mathcal{T}_n}{N} - \frac{\Gamma(n+1/2)}{\sqrt{\pi}\Gamma(n+1)}\right]^2\right\}$$
$$(13)$$

from which one easily reads off the mean and variance of integer moments

$$\langle\mathcal{T}_n\rangle = \frac{N\Gamma(n+1/2)}{\sqrt{\pi}\Gamma(n+1)}, \qquad (14)$$

$$\text{var}(\mathcal{T}_n) = \frac{2}{\beta b_n} = \frac{[\Gamma(n+1/2)]^2}{2\beta\pi\Gamma(n)\Gamma(n+1)}. \qquad (15)$$

To the best of our knowledge, the latter result, together with its universal asymptotic value $\lim_{n\to\infty}\text{var}(\mathcal{T}_n)=(2\beta\pi)^{-1}$, has not been reported previously in the literature.

As in the case of conductance and shot noise, there are singular points separating the central Gaussian regime and the non-Gaussian tails. However, the situation is more complicated for $n>1$. Unlike in the conductance or the shot-noise case where there are only two phase transitions separating three regimes, there are more regimes for $n>1$. We analyze here in detail the case $n=2$ where we show that there are actually three singular points separating four regimes. This is again a consequence of phase transitions in the associated Coulomb gas problems where the average charge density undergoes abrupt changes at these critical points. It would be interesting to see how many such phase transitions occur for $n>2$. However, we do not have any simple way to predict this and this remains an interesting open problem. The tails of the distribution for the integer moments case can be computed, in principle, for general $n>1$, and the formalism is developed in Sec. VI, but for clarity we will focus mostly on the case $n=2$. The left tail has again a power-law decay for any $n>1$.

III. SUMMARY OF THE COULOMB GAS METHOD

It is useful to summarize briefly the method we use to compute the distribution of linear statistics in the large N limit. Given a linear statistics of interest $A = \sum_{i=1}^{N} a(T_i)$, its pdf $\mathcal{P}_A(A,N)$, using the joint pdf of T_i's in Eq. (2), is given by

$$\mathcal{P}_A(A,N) = A_N \int_0^1 \ldots \int_0^1 dT_1, \ldots, dT_N \exp\left[\frac{\beta}{2} \sum_{j \neq k} \log|T_j - T_k| \right.$$
$$\left. + \left(\frac{\beta}{2} - 1 \right) \sum_{i=1}^{N} \log T_i \right] \delta\left[\sum_{i=1}^{N} a(T_i) - A \right]. \quad (16)$$

The main idea then is to work with its Laplace transform

$$\mathbf{F}_N(z;A) = \int_0^\infty dA \mathcal{P}_A(A,N) e^{-(\beta/2)zA}, \quad (17)$$

where the variable z takes, in principle, complex values and its dependence on N is at present unspecified.

Suppose one is able to compute the following limit:

$$J_A(p) = -\frac{2}{\beta} \lim_{N \to \infty} \frac{\log \mathbf{F}_N(N^\alpha p;A)}{N^2} \quad (18)$$

and such limit is finite and nonzero for a certain *speed* α and for $p \in \mathbb{R}$ such that $p \sim \mathcal{O}(1)$ for $N \to \infty$. It is then a classical result in large deviation theory (Gärtner-Ellis theorem, see, e.g., Ref. 55, Appendix C) that the following finite nonzero limit exists:

$$\Psi_A(x) = -\frac{2}{\beta} \lim_{N \to \infty} \frac{\log \mathcal{P}_A(N^\alpha x, N)}{N^2} \quad (19)$$

and $\Psi_A(x)$ (the *rate function*) is given by the inverse Legendre transform of $J_A(p)$

$$\Psi_A(x) = \max_p [J_A(p) - px]. \quad (20)$$

Note that

(1) there is no need to consider *complex* values for z (and thus for p) in Eq. (17), as only real values matter for obtaining the rate function. As $\mathcal{P}_A(A,N)$ has generically a compact support, negative values for p are also allowed.

(2) Setting the appropriate speed α is evidently *crucial* for obtaining a finite nonzero limit in Eq. (18). There is no freedom here. Conversely, *any* speed is equally good when extracting the *cumulants* out of the Laplace transform, Eq. (17), ($z = N^\alpha p$) through the formula (set $\beta = 2$ for simplicity)

$$\kappa_\ell(A) = \left(\frac{-1}{N^\alpha} \right)^\ell \frac{\partial^\ell}{\partial p^\ell} \log \mathbf{F}_N(N^\alpha p;A)\big|_{p=0} \quad (21)$$

as no limiting procedure is performed in Eq. (21).

(3) The rate function $\Psi_A(x)$ encodes the full information about the probability distribution in the limit of infinitely many open channels. However, our numerical simulations confirm that it also gives a fairly accurate description of such distribution for rather small N.

What is then the correct speed α for the linear statistics considered here? It is quite easy to argue that α must be set equal to 1. The reason is best understood by taking the conductance $G = \sum_{i=1}^{N} T_i$ for $\beta = 2$ as an example. By very general arguments we expect the large N behavior of $\mathcal{P}_G(G,N)$ to scale as $\mathcal{P}_G(G,N) \sim e^{-N^2 \Psi_G(G/N)}$ for large N. Clearly, the two exponentials in Eq. (17) [the one coming from $\mathcal{P}_G(G,N)$ and the other coming from the Laplace measure] must be of the same order in N to guarantee a meaningful saddle point contributions and since $G \sim N$ for large N, clearly $z \sim N$ as well.

After setting the proper speed, we get in full generality

$$\underbrace{\int_0^\infty \mathcal{P}_A(A,N) e^{-(\beta/2)NpA} dA}_{\mathbf{F}_N(Np;A)} = A_N \int_0^1 \ldots \int_0^1 dT_1 \ldots dT_N \exp\left[\frac{\beta}{2} \sum_{j \neq k} \log|T_j - T_k| + \left(\frac{\beta}{2} - 1 \right) \sum_{i=1}^{N} \log T_i - \frac{\beta}{2} pN \sum_{i=1}^{N} a(T_i) \right].$$

$$(22)$$

We can write the exponential as, $\exp[-\beta E(\{T_i\})]$ with $E(\{T_i\}) = -(1/2)\sum_{j \neq k} \log|T_j - T_k| + \sum_i V(T_i)$ where $V(T) = (1/\beta - 1/2)\log(T) + pNa(T)/2$. This representation provides a natural Coulomb gas interpretation. We can identify T_i's as the coordinates of the charges of a two-dimensional (2D) Coulomb gas that lives on a one-dimensional real segment [0,1]. The charges repel each other via the 2D logarithmic Coulomb potential and in addition, they sit in an external potential $V(T)$. Note that the Laplace parameter p appears explicitly in the external potential $V(T)$. Then E is the energy of this Coulomb gas. Thus one can write the Laplace transform as the ratio of two partition functions

$$\mathbf{F}_N(Np;A) = \int_0^\infty \mathcal{P}_A(A,N) e^{-(\beta/2)NpA} dA = \frac{Z_p(N)}{Z_0(N)}, \quad (23)$$

where $Z_p(N)$ is precisely the multiple integral on the rhs of Eq. (22) and $Z_0(N) = 1/A_N$ [which simply follows by putting $p = 0$ in Eq. (22) and using the fact that the pdf $\mathcal{P}_A(A,N)$ is normalized to unity].

The next step is to evaluate this partition function $Z_p(N)$ of the Coulomb gas in the large N limit. This procedure for the large N calculation was originally introduced by Dyson[19] and has recently been used in the context of the largest eigenvalue distribution of Gaussian[45] and Wishart random matrices[53] and also in other related problems of counting

stationary points in random Gaussian landscapes.[46] There are two basic steps involved. The first step is a coarse-graining procedure where one sums over (partial tracing) all microscopic configurations of T_i's compatible with a fixed charge-density function $\varrho_p(T) = N^{-1} \Sigma_i \delta(T - T_i)$ and the second step consists in performing a functional integral over all possible positive charge densities $\varrho_p(T)$ that are normalized to unity. Finally the functional integral is carried out in the large N limit by the saddle-point method.

Following this general procedure summarized in Ref. [45] the resulting functional integral, to leading order in large N, becomes

$$Z_p(N) \propto \int \mathcal{D}[\varrho_p] e^{-(\beta/2)N^2 S[\varrho_p]}, \qquad (24)$$

where the action is given by

$$S[\varrho_p] = p \int_0^1 \varrho_p(T) a(T) dT + B\left[\int_0^1 \varrho_p(T) dT - 1\right]$$
$$- \int_0^1 \int_0^1 dT dT' \varrho_p(T) \varrho_p(T') \log|T - T'|. \qquad (25)$$

Here B is a Lagrange multiplier enforcing the normalization of $\varrho_p(T)$. Note that the part of the potential $(1/\beta - 1/2)\Sigma_i \log(T_i)$ is of $\mathcal{O}(N)$ and hence it drops out of the action in Eq. (25) in the large N limit. In the large N limit, the functional integral in Eq. (24) is particularly suitable to be evaluated by the saddle point method,[56] i.e., one finds the solution $\varrho_p^\star(T)$ (the equilibrium charge density that minimizes the action or the free energy) from the stationarity condition $\delta S[\varrho_p]/\delta \varrho_p = 0$ which leads to an integral equation

$$V_{\text{ext}}(T) = pa(T) + B = 2 \int_0^1 \varrho_p^\star(T') \log|T - T'| dT', \quad (26)$$

where $V_{\text{ext}}(T) = pa(T) + B$ is termed as external potential. Differentiating once with respect to T leads to a singular integral equation

$$\frac{p}{2} a'(T) = \text{Pr} \int_0^1 \frac{\varrho_p^\star(T')}{T - T'} dT', \qquad (27)$$

where Pr denotes the principal part and $a'(T) = da/dT$.

Assuming one can solve Eq. (27) for $\varrho_p^\star$, one next evaluates the action $S[\varrho_p]$ in Eq. (25) at the stationary solution $\varrho_p^\star$ and then takes the ratio in Eq. (23) to get [upon comparison with Eq. (18)]

$$\underbrace{\int_0^\infty \mathcal{P}_A(A,N) e^{-(\beta/2)NpA} dA}_{\mathbf{F}_N(Np;A)} \approx e^{-(\beta/2)N^2 \overbrace{[S[\varrho_p^\star] - S[\varrho_0^\star]]}^{J_A(p)}}. \qquad (28)$$

Inverting the Laplace transform gives the main asymptotic result $\mathcal{P}(A,N) \approx \exp[-\frac{\beta}{2}N^2 \Psi_A(\frac{A}{N})]$ where the rate function is the inverse Legendre transform [see Eq. (20)]

$$\Psi_A(x) = \max_p [-xp + J_A(p)] \qquad (29)$$

with $J_A(p)$ given by the *free-energy difference* as in Eq. (28).

To summarize, given any linear statistics $a(T)$, the steps are: (i) solve the singular integral Eq. (27) for the density $\varrho_p^\star(T)$ (ii) evaluate the action $S[\varrho_p^\star]$ in Eq. (25), (iii) evaluate $J_A(p) = S[\varrho_p^\star] - S[\varrho_0^\star]$, and finally (iv) use $J_A(p)$ in Eq. (29), maximize the rhs to evaluate the rate function $\Psi_A(x)$. We will see later that all these steps can be carried out fully and explicitly when $A = G$ (conductance) and $A = P$ (shot noise) and partially when $A = \mathcal{T}_n$ (integer moments).

The important first step is to find the explicit solution of the singular integral Eq. (27). Note that this equation is of the Poisson form and it is, in some sense, an inverse electrostatic problem: given the potential $pa'(T)/2$ on the l.h.s. of Eq. (27), we need to find the charge density $\varrho_p^\star(T)$. To proceed, we recall a theorem due to Tricomi[57] concerning the general solution to singular integral equations of the form

$$g(x) = \text{Pr} \int_a^b \frac{f(x')}{x - x'} dx', \qquad (30)$$

where $g(x)$ is given and one needs to find $f(x)$ which has only a single support over the interval $[a, b]$ with $a < b$ [the lower edge a should not be confused with the linear statistics function $a(T)$]. The solution $f(x)$, with a single support over $[a, b]$ can be found explicitly[57]

$$f(x) = -\frac{1}{\pi^2 \sqrt{(b-x)(x-a)}}$$
$$\times \left[\text{Pr} \int_a^b \frac{\sqrt{(b-x')(x'-a)}}{x - x'} g(x') dx' + B_1\right], \quad (31)$$

where B_1 is an arbitrary constant.

In our case, $g(x) = pa'(x)/2$ and provided we assume that the charge density has a single support over $[a, b]$ with $a < b$, we can, in principle, use this solution, Eq. (31). However, if the solution happens to have a disconnected support one cannot use this formula directly. Whether the solution has a single or disconnected support depends, of course, on the function $a(T)$. We will see that indeed for the case of conductance $[a(T) = T]$, the solution has a single support and one can use Eq. (31) directly. The edges a and b in that case are determined self-consistently as explained in Sec. IV. On the other hand, for the shot noise $[a(T) = T(1-T)]$ and for integer moments with $n > 1$ $[a(T) = T^n]$, it turns out that for certain values of the parameter p, the solution has a disconnected support. In that case, one cannot use Eq. (31) directly. However, we will see later that one can still obtain the solution explicitly by an indirect application of Eq. (31).

A very interesting feature of Eq. (27) is that, depending on the value of the Laplace parameter p, the fluid of charged particles undergoes a series of real phase transitions in Laplace space, i.e., as one varies the Laplace parameter p, there are certain critical values of p at which the solution $\varrho_p^\star(T)$ abruptly changes its form. As a consequence, the rate function, related to the Laplace transform via the Legendre transform in Eq. (29), also undergoes a change in behavior as
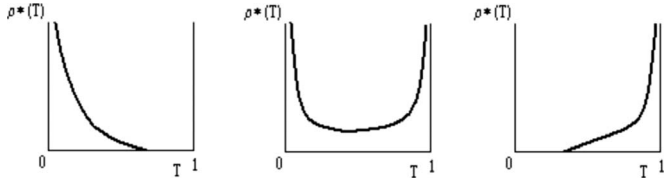
FIG. 2. Phases of the density of transmission eigenvalues for the conductance case.

one varies its argument at the corresponding critical points. The rate function is continuous at these critical points but it has weak nonanaliticities (characterized by a discontinuous third derivative).

As an example, we consider the case of the conductance $[a(T)=T]$ (see Sec. IV for details). In Fig. 2, we plot schematically the saddle point density $\varrho_p^\star(T)$ [solution of Eq. (27) with $a(T)=T$], for three different intervals on the real p line. We will see in the next section that there are three possible solutions valid respectively for $p \geq 4$, $-4 \leq p \leq 4$, and $p \leq -4$.

(1) When $p \geq 4$, the external potential $V_{\text{ext}}(T)=pT+B$ is strong enough (compared to the logarithmic repulsion) to keep the fluid particles confined between the hard wall at $T=0$ and a point $L_1=4/p$. The gas particles accumulate toward $T \to 0^+$, where the density develops an inverse square root divergence, while $\varrho_p^\star(L_1)=0$. This situation is depicted in the left panel of Fig. 2;

(2) when p hits the critical value $p^{(+)}=4$ from above, the density profile changes abruptly. The external potential V_{ext} is no longer overcoming the logarithmic repulsion so the fluid particles spread over the whole support (0,1) and the density generically exhibits an inverse square root divergence at both end points ($T \to 0^+$ and $T \to 1^-$). This phase keeps holding for all the values of p down to the second critical point $p^{(-)}=-4$ (see the second panel in Fig. 2), when the negative slope of the potential is so steep that the particles can no longer spread over the whole support (0,1) but prefer to be located near the right hard edge at $T=1$.

(3) In the third phase ($p < -4$), the fluid particles are pushed away from the origin and accumulate toward the right hard wall at $T \to 1$ (see the rightmost panel in Fig. 2). The density thus vanishes below the point $L_2=1-4/|p|$.

It is worth mentioning that such phase transitions in the solutions of integral equations have been observed recently in other systems that also allow similar Coulomb gas representations. These include bipartite quantum-entanglement problem,[58] nonintersecting fluctuating interfaces in presence of a substrate,[49] and also multiple input multiple output channels.[59]

IV. DISTRIBUTION OF THE CONDUCTANCE

We start with the simplest case of linear statistics, namely, the conductance $G = \sum_{i=1}^{N} T_i$. Thus in this case $a(T)=T$ is simply a linear function. Substituting $a(T)=T$ in Eq. (26) gives

$$V_{\text{ext}}(T) = pT + B = 2 \int_0^1 \varrho_p^\star(T') \log|T-T'| dT' \qquad (32)$$

and then Eq. (27) becomes

$$\frac{p}{2} = \text{Pr} \int_0^1 \frac{\varrho_p^\star(T')}{T-T'} dT' . \qquad (33)$$

We have then to find the solution to Eq. (33). Once this solution $\varrho_p^\star(T)$ is found, we can evaluate the action $S[\varrho_p^\star]$ at the saddle point in the following way. Multiplying Eq. (32) by $\varrho_p^\star(T)$ and integrating [using the normalization $\int_0^1 \varrho_p^\star(T)dT=1$] gives

$$p \int_0^1 T\varrho_p^\star(T)dT + B = 2 \int_0^1 \int_0^1 \varrho_p^\star(T)\varrho_p^\star(T')$$
$$\times \log|T-T'|dTdT' . \qquad (34)$$

Next we use this result to replace the double integral term in the action in Eq. (25) [with $a(T)=T$] to get

$$S[\varrho_p^\star] = \frac{p}{2} \int_0^1 \varrho_p^*(T)TdT - \frac{B}{2} . \qquad (35)$$

The yet unknown constant B is determined from Eq. (32) upon using the explicit solution, once found.

To find the solution to Eq. (33) explicitly we will use the general Tricomi formula in Eq. (31) assuming a connected support over $[a,b]$. The edges a and b will be determined self-consistently. Physically, we can foresee three possible forms for the density $\varrho_p^\star(T)$ according to the strength and sign of the external potential $V_{\text{ext}}(T)=pT+B$ on the left-hand side of Eq. (32).

(1) For large and positive p, the fluid particles (transmission eigenvalues) will feel a strong confining potential which keeps them close to the left hard edge $T \to 0+$. Thus, $\varrho_p^\star(T)$ will have a support $[0,L_1]$ with $0 < L_1 < 1$.

(2) For intermediate values of p, the particles will spread over the full range $[0,1]$.

(3) For large and negative p, the fluid particles will be pushed toward the right edge and the support of $\varrho_p^\star(T)$ will be over $[L_2,1]$ with $0 < L_2 < 1$.

These three cases will correspond to different solutions for the Tricomi Eq. (33) above and the positivity constraint for the obtained densities will fix the range of variability for p in each case. Once a solution $\varrho_p^\star(T)$ for each case (different ranges for p) is obtained, we can then use Eq. (35) to evaluate the action at the saddle point. Let us consider the three cases discussed above separately.

A. Large p: support on $[0,L_1]$

We assume that the solution is nonzero over the support $[0,L_1]$ based on our physical intuition for large p, where L_1 is yet unknown. We use the general Tricomi solution with a single support in Eq. (31) with $a=0$, $b=L_1$, and $g(x)=p/2$ giving
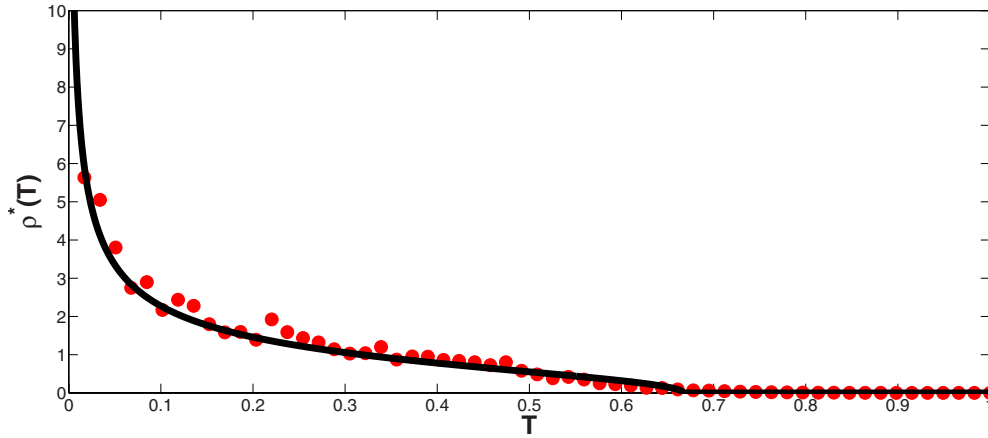
FIG. 3. (Color online) Density of transmission eigenvalues T for $N=5$ and $p=6$ (theory vs numerics) for the conductance case.

$$\varrho_p^\star(T) = -\frac{1}{\pi^2\sqrt{T(L_1-T)}}\left[\frac{p}{2}\mathrm{Pr}\int_0^{L_1}\frac{\sqrt{T'(L_1-T')}}{T-T'}dT' + B_1\right],$$
(36)

where B_1 is an arbitrary constant. Evaluating the principal value integral on the rhs of Eq. (36) we get

$$\varrho_p^\star(T) = \frac{p}{2\pi\sqrt{T}}\sqrt{L_1-T},$$
(37)

where the constant B_1 has been determined using the fact that the density $\varrho_p^\star(T)$ must vanish at the upper edge $T=L_1$. The normalization of $\varrho_p^\star(T)$ gives

$$L_1 = \frac{4}{p}, \quad L_1 < 1 \Rightarrow p > 4.$$
(38)

As expected, this solution holds for large values of p (i.e., for a strong confining potential).

Since the point $T=0$ belongs to the support $[0,L_1]$, we can put $T=0$ in Eq. (32) to determine the constant B

$$B = 2\int_0^1 \varrho_p^\star(T')\log T' dT'.$$
(39)

Substituting B in Eq. (35) gives the saddle-point action

$$S[\varrho_p^\star] = \frac{p}{2}\int_0^1 \varrho_p^\star(T)T dT - \int_0^1 \varrho_p^\star(T)\log(T)dT.$$
(40)

Performing the integrals using the explicit solution $\varrho_p^\star(T)$ Eq. (37) gives a very simple expression, valid for $p>4$

$$S[\varrho_p^\star] = 3/2 + \log p.$$
(41)

In Fig. 3 we show the results from a Monte Carlo simulation to test the prediction Eq. (37) for the average density of eigenvalues in Laplace space for $p>4$. The numerical density for N eigenvalues (here and for all the subsequent cases) is obtained as

$$\varrho_p^\star(x_1) \simeq \frac{\left\langle e^{-pN\Sigma_{i=1}^N x_i}\prod_{j<k}|x_j-x_k|^2\right\rangle_{N-1}}{\left\langle e^{-pN\Sigma_{i=1}^N x_i}\prod_{j<k}|x_j-x_k|^2\right\rangle_N},$$
(42)

where the average $\langle\cdot\rangle$ is taken over $N-1$ random numbers $x_2,\ldots,x_N$ (numerator) with a flat measure over $[0,1]$ with x_1 spanning the interval $(0,1)$. In the denominator, the normalization constant is obtained with the same procedure, this time averaging over N random variables uniformly drawn from $(0,1)$. In all cases, the agreement with the theoretical results is fairly good already for $N=5$.

B. Intermediate p: support on the full range (0,1)

In this case, the solution of Eq. (33) from Eq. (31) reads

$$\varrho_p^\star(T) = \frac{p}{2\pi\sqrt{T(1-T)}}[K-T].$$
(43)

The normalization of $\varrho_p^\star(T)$ determines $K=(4+p)/2p$. Now, depending on whether $p>0$ or $p<0$, there are two positivity constraints $[\varrho_p^\star(T)>0$ everywhere$]$ to take into account:

(1) If $p>0$, the positivity constraint $K-1>0$ at the upper edge $T=1$ implies $p<4$.

(2) If $p<0$, the positivity constraint $K<0$ at the lower edge $T=0$ implies $p>-4$. Thus the solution in Eq. (43) with support over the full allowed range $(0,1)$ is valid for all $-4\leq p\leq 4$.

Substituting this solution into the simplified action in Eq. (40) (which holds in this case as well) gives

$$S[\varrho_p^\star] = -\frac{p^2}{32} + \frac{p}{2} + 2\log 2.$$
(44)

Note that since this range $-4\leq p\leq 4$ includes, in particular, the $p=0$ case, we can use the expression in Eq. (44) to evaluate the value of the action at $p=0$ that will be required later in evaluating the large deviation function via Eq. (28). Putting $p=0$ in Eq. (44) gives

$$S[\varrho_0^\star] = 2\log 2.$$
(45)

In Fig. 4, we plot the analytical result for the density together with Monte Carlo simulations for $N=5$ and $p=1$.
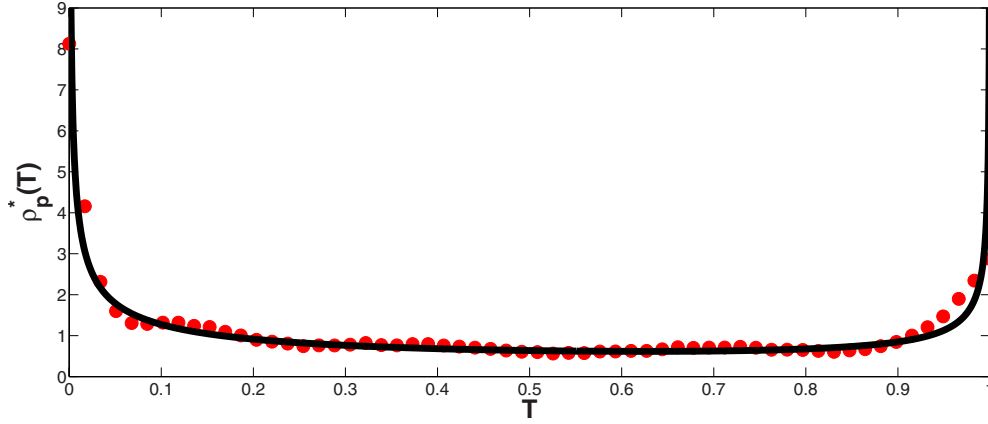
FIG. 4. (Color online) Density of transmission eigenvalues T for $N=5$ and $p=1$ (theory vs numerics) for the conductance case.

C. Large negative p: support on $[L_2, 1]$

In this case, the solution of Eq. (33) reads

$$\varrho_p^\star(T) = \frac{|p|}{2\pi\sqrt{1-T}}\sqrt{T-L_2}, \quad L_2 = 1 - \frac{4}{|p|}. \tag{46}$$

The implications for the p range are as follows:

$$L_2 > 0 \Rightarrow p < -4. \tag{47}$$

Note that we can no longer use the expression for the constant B in Eq. (39) since now the allowed range of the solution $[L_2, 1]$ does not include the point $T=0$. Instead, putting $T=1$ in Eq. (32), we determine the value of B as

$$B = 2\int_0^1 \varrho_p^\star(x')\log|1-x'|dx' - p. \tag{48}$$

Substituting B in Eq. (35) we get a new expression for the action at the saddle point

$$S[\varrho_p^\star] = \frac{p}{2}\int_0^1 dT\, T\varrho_p^\star(T) - \int_0^1 dT\varrho_p^\star(T)\log|1-T| + \frac{p}{2}. \tag{49}$$

Evaluating Eq. (49) using the solution in Eq. (46) gives the saddle-point action for $p < -4$

$$S[\varrho_p^\star] = 3/2 + p + \log(-p). \tag{50}$$

In Fig. 5, we plot the analytical result for the density together with Monte Carlo simulations for $N=5$ and $p=-6$.

D. Comparison with other theories and numerical simulations

As summarized in the next section, we obtained for the rate function of the conductance for $\beta=2$, defined as [see Eq. (19)]

$$\Psi_G(x) = -\lim_{N\to\infty}\frac{\log \mathcal{P}_G(Nx,N)}{N^2} \tag{51}$$

the following expression [limited to $x \in [1/2, 1]$, given the symmetry $\Psi_G(x) = \Psi_G(1-x)$]:

$$\Psi_G(x) = \begin{cases} 8\left(x-\frac{1}{2}\right)^2 & 1/2 \le x \le 3/4 \\ \frac{1}{2} - \log[4(1-x)] & 3/4 \le x < 1. \end{cases} \tag{52}$$

Osipov and Kanzieper (OK) claim[40] a different limiting law, namely,
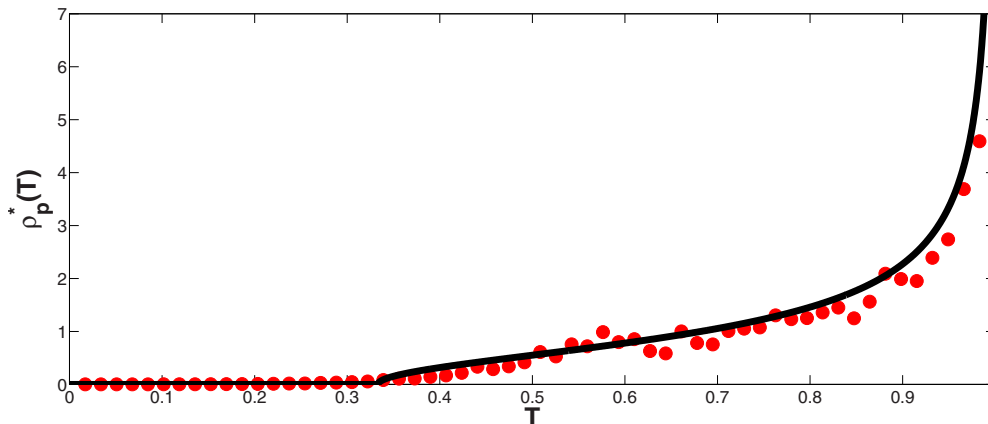

FIG. 5. (Color online) Density of transmission eigenvalues T for $N=5$ and $p=-6$ (theory vs numerics) for the conductance case.
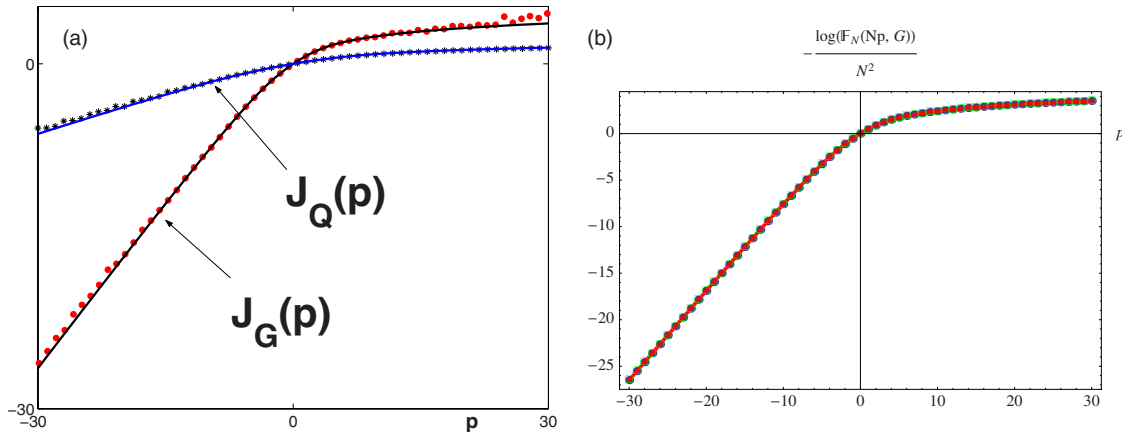
FIG. 6. (Color online) Left: $J_G(p)$ and $J_Q(p)$ vs Monte Carlo simulations [see Eqs. (70) and (80)]. Right: our asymptotic predictions $J_G(p)$ (solid red line) is compared with the exact finite N expression (59) from Ref. 40 for $N=4$ (green squares) and $N=10$ (blue dots). Already for $N=4$, our large N formula again matches the exact finite N result with accuracy up to the second decimal digit over the full real p range.

$$\Psi_G^{\text{OK}}(x) = \begin{cases} 8\left(x - \dfrac{1}{2}\right)^2 & 1/2 \leq x \leq 3/4 \\ \\ 4x - \dfrac{5}{2} & 3/4 \leq x < 1 \end{cases} \quad (53)$$

and $\Psi_G^{\text{OK}}(x)$ would approach the form in Eq. (52) (second line) only at the extreme edge $x \to 1^-$ (over a narrow region of order $1/N$).

Which law is then correct? There is a conclusive way to settle this dispute, namely, to compare the two theoretical results to a direct numerical simulation of $\mathcal{P}_G(G,N)$. We will present simulation results in Laplace space which agree very well with our result on the Laplace transform [see Fig. 6, left panel, and Eqs. (65) and (70) in next section] *over the full range of real p* values, as well as a convincing comparison with the *exact* finite N result for the same observable using the Hankel determinant representation in Eq. (59) from Ref. 40 (see Fig. 6, right panel). We shall argue below that OK asymptotic theory is indeed unable to reproduce the tails of $J_G(p)$ for $|p| > 4$, which are responsible for long power-law tails in the rate function $\Psi_G(x)$. Since, however, working in the Laplace space may not appear conclusive as far as the real-space rate function $\Psi_G(x)$ is concerned, it would be better if one could perform a simulation directly for $\mathcal{P}_G(G,N)$ and not just for its Laplace transform. Indeed, it turns out to be quite easy to simulate directly $\mathcal{P}_G(G,N)$ using an elementary and standard Monte Carlo Metropolis algorithm which we describe below.

Monte-Carlo method

The main problem is to compute the distribution of the conductance G which, for a fixed number of channels N and $\beta=2$, is given by the multiple integral

$$\mathcal{P}_G(G,N) = A_N \int_0^1 \prod_{i=1}^N dT_i \prod_{i<j} (T_i - T_j)^2 \delta\left(\sum_{i=1}^N T_i - G\right), \quad (54)$$

where the prefactor A_N is set by the normalization: $\int_0^\infty \mathcal{P}_G(G,N)dG = 1$ and is known exactly for all N [see Eq. (3)].

To employ the Monte Carlo method, we first write the integrand (the Vandermonde term) in Eq. (54)

$$\prod_{i<j} (T_i - T_j)^2 = e^{-E\{T_i\}}; \quad E\{T_i\} = -\sum_{i \neq j} \ln(|T_i - T_j|). \quad (55)$$

Thus, one can interpret $0 \leq T_i \leq 1$ as the position of an ith charge in a one-dimensional box $[0,1]$ and the charges interact via the logarithmic Coloumb energy $-E\{T_i\}$. This Coulomb gas is in thermal equilibrium with a Gibbs weight $\exp[-E\{T_i\}]$ for any configuration $\{T_i\}$, where the inverse temperature is set to 1.

It is then very easy and standard to simulate the equilibrium properties of this gas via a Monte Carlo method.[60] We start from any configuration $\{T_i\}$. We pick a particle, say the ith one, at random and attempt to move its position by an amount δ: $T_i \to T_i + \delta$. This move causes a change in energy ΔE of the gas. According to the standard Metropolis algorithm,[60] the move is accepted with probability $e^{-\Delta E}$ if $\Delta E > 0$ and with probability 1 if $\Delta E < 0$. The move is rejected if the new position $T_i + \delta$ is outside the box $[0,1]$. This Metropolis move guarantees that after a large number of microscopic moves, the system reaches the stationary distribution with the correct Boltzmann weight $e^{-E\{T_i\}}$.

We wait for a long enough time to ensure that the system has indeed reached equilibrium. After that we let the system evolve according to these microscopic moves and construct the normalized histogram $\mathcal{P}_G(G,N)$ of $G = \Sigma_{i=1}^N T_i$. Once again, we are guaranteed that T_i's are sampled with the correct equilibrium weight. This procedure allows us to simulate fairly large systems. To obtain good statistics for the distribution over the full range of $x = G/N$, i.e., over $1/2 \leq x \leq 1$, we implement an iterative conditional sampling method, used in other contexts before,[51] that allows us to generate events with extremely small probabilities at the far tail of the distribution.[61]

In Fig. 7, we plot $\Psi(x) = -\ln[\mathcal{P}_G(G,N)]/N^2$ vs the scaling variable $x = G/N$ for $1/2 \leq x \leq 1$ for $N=50$. The black dots show the simulation points. The red (solid) line shows our Vivo-Majumdar-Bohigas (VMB) result in Eq. (52) while the blue (dashed) line shows the OK prediction, Eq. (53).
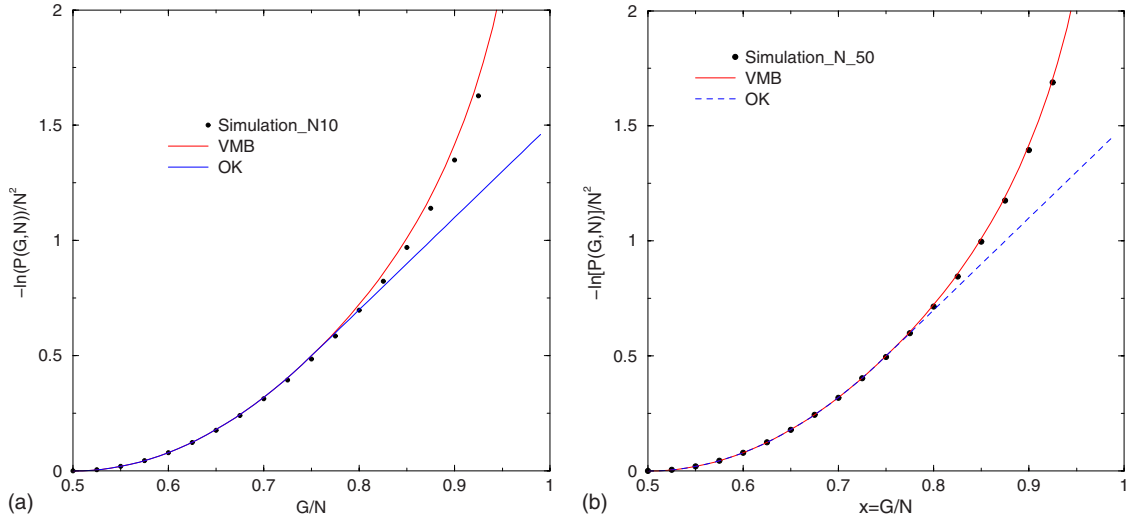
FIG. 7. (Color online) Comparison between Montecarlo simulations for the rate function $\Psi(x) = -\lim_{N\to\infty} \log \mathcal{P}_G(Nx, N)/N^2$ as a function of $x = G/N$ for $\beta = 2$ (black dots), our asymptotic theory (VMB) (continuous red line) and the theory by OK (dashed blue line). Simulations are performed for $N = 10$ (left) and $N = 50$ (right), which allows to appreciate the convergence to our theoretical curve as N is increased.

Clearly the two results agree with each other, as well as with the simulations, in the Gaussian regime $1/2 \leq x \leq 3/4$. However, in the outer region $3/4 \leq x < 1$ while the VMB result in Eq. (52) is in perfect agreement with the simulation results, the OK result in Eq. (53) deviates widely from them. *This proves conclusively that in the regime $3/4 \leq x < 1$, the VMB result in Eq. (52) is correct and the OK result in Eq. (53) is incorrect.*

There is another way to see that the OK asymptotics cannot be correct. Since OK theory stems from the asymptotic analysis of the following integral representation for the probability distribution of conductance (see Eq. 22 of Ref. 40):

$$\mathcal{P}_G^{(OK)}(G, N) = \frac{2N^{1/4}}{\Gamma(1/8)} \sqrt{\frac{2}{\pi}} \int_0^\infty d\lambda \frac{e^{-N^2[\lambda + 2\eta^2/(1+2\lambda)]}}{\lambda^{7/8}\sqrt{1+2\lambda}},$$
(56)

where $\eta = 2(G/N) - 1$, we can now compute from Eq. (56) the *same* observable we considered here, namely,

$$J_G(p) = -\lim_{N\to\infty} \frac{\log \mathbf{F}_N(Np; G)}{N^2}$$
(57)

for $p \in \mathbb{R}$ and $p \sim \mathcal{O}(1)$ for $N \to \infty$ [see Eqs. (17) and (18)], and thus compare once again the large N predictions of VMB and OK theories against (i) numerical simulations and (ii) the exact finite N result, which is fortunately available (see Fig. 6).

Inserting Eq. (56) into the definition of the Laplace transform in Eq. (17), we obtain after simple algebraic steps

$$\mathbf{F}_N(Np; G) = \frac{N^{1/4}}{\Gamma(1/8)} \exp\left[-N^2\left(\frac{p}{2} - \frac{p^2}{32}\right)\right]$$
$$\times \underbrace{\int_0^\infty d\lambda \frac{e^{-N^2\lambda(1-p^2/16)}}{\lambda^{7/8}}}_{\phi_N(p)}.$$
(58)

The integral $\phi_N(p)$ clearly does not converge for $|p| \geq 4$ with the consequence that OK integral representation in Eq. (56) fails to reproduce the tails of both (1) Monte Carlo simulations of $J_G(p)$ (see Fig. 6, left panel) and (2) the exact finite N result[40] for the Laplace transform in terms of a Hankel determinant (see Fig. 6, right panel)

$$\mathbf{F}_N(Np; G) = \frac{N!}{c_N}\det\left[(-\partial_z)^{j+k}\frac{1-e^{-z}}{z}\bigg|_{z=Np}\right]_{0\leq j,k\leq N-1},$$
$$c_N = \prod_{j=0}^{N-1} \frac{\Gamma(j+2)\Gamma^2(j+1)}{\Gamma(j+N+1)},$$
(59)

which evidently *do* exist and are perfectly captured instead by our approach in both cases.

*Within the range of validity $|p| < 4$, the integral $\phi_N(p)$ can be evaluated and gives eventually

$$\mathbf{F}_N(Np; G) = \frac{\exp[-N^2(p/2 - p^2/32)]}{(1-p^2/16)^{1/8}}, \quad \text{if } |p| < 4.$$
(60)

Note that *all N* dependence has completely dropped out from the prefactor, leaving us with two perfectly compatible (even though apparently discordant at first glance) consequences:

(1) according to OK theory, the limit

$$J_G(p) = -\lim_{N\to\infty} \frac{\log \mathbf{F}_N(Np; G)}{N^2} = p/2 - p^2/32 \quad \text{for } |p| < 4,$$
(61)

which is correct but incomplete (as their integral has nothing to say about the tails $|p| \geq 4$).

(2) Not surprisingly then, from the OK theory, the leading $(1/N)$ order of the cumulants of the distribution, computed through the formula (21)

$$\kappa_\ell(G) = \left(\frac{-1}{N}\right)^\ell \frac{\partial^\ell}{\partial p^\ell} \log \mathbf{F}_N(Np;G)\big|_{p=0} \qquad (62)$$

is correctly reproduced (see also Ref. 39 for an independent calculation of such cumulants, which is in perfect agreement with OK result).

In summary, the OK integral representation in Eq. (56) is only adequate around the Gaussian peak [the $p=0$ neighborhood in Laplace space, *which is exactly the only region which cumulants probe*, see Eq. (62)] and in this neighborhood it has the merit of producing the correct leading $1/N$ term of the expansion of such cumulants (unattainable by our method) and confirmed independently in Ref. 39. Outside

this region, however, the OK integral representation is invalid and the asymptotic analysis of it *outside its range of validity* obviously produces an incorrect result. Note also that, for any fixed N (however large), one has from Eq. (56) that $\mathcal{P}_G^{(OK)}(G=0,N) = \mathcal{P}_G^{(OK)}(G=N,N) > 0$ strictly while it is well known that the density must vanish identically at the edges[38,39,54] *for any N*. This simple observation rules out the claims of exactness of Eq. (56) in Ref. 40.

E. Final results for the conductance case

To summarize, the density of eigenvalues [solution of the saddle point Eq. (33)] has the following form:

$$\varrho_p^\star(T) = \begin{cases} \dfrac{p}{2\pi\sqrt{T(1-T)}}\left[\dfrac{4+p}{2p} - T\right] & 0 \le T \le 1 & -4 \le p \le 4 \\[3ex] \dfrac{p}{2\pi\sqrt{T}}\sqrt{\dfrac{4}{p} - T} & 0 \le T \le 4/p & p \ge 4 \\[3ex] \dfrac{|p|}{2\pi\sqrt{1-T}}\sqrt{T - (1-4/|p|)} & 1-4/|p| \le T \le 1 & p \le -4. \end{cases} \qquad (63)$$

One may easily check that $\varrho_p^\star(T)$ is continuous at $p = \pm 4$ but develops two phase transitions characterized by different supports.

The action at the saddle point is given by

$$S[\varrho_p^\star] = \begin{cases} -\dfrac{p^2}{32} + \dfrac{p}{2} + 2\log 2 & -4 \le p \le 4 \\[2ex] 3/2 + \log p & p \ge 4 \\[1ex] 3/2 + p + \log(-p) & p \le -4, \end{cases} \qquad (64)$$

which is again continuous at $p = \pm 4$.

Using the above expressions for the saddle point action and the result in Eq. (45), the expression for the free-energy difference $J_G(p) = S[\varrho_p^\star] - S[\varrho_0^\star]$ follows from Eq. (28)

$$J_G(p) = \begin{cases} -\dfrac{p^2}{32} + \dfrac{p}{2} & -4 \le p \le 4 \\[2ex] 3/2 + \log(p/4) & p \ge 4 \\[1ex] 3/2 + p + \log(-p/4) & p \le -4. \end{cases} \qquad (65)$$

Using this expression for $J_G(p)$ in the Legendre transform in Eq. (29) and maximizing gives the exact expression for the rate function

$$\Psi_G(x) = \begin{cases} 8\left(x - \dfrac{1}{2}\right)^2 & \dfrac{1}{4} \le x \le \dfrac{3}{4} \\[2ex] \dfrac{1}{2} - \log(4x) & 0 \le x \le \dfrac{1}{4} \\[2ex] \dfrac{1}{2} - \log[4(1-x)] & \dfrac{3}{4} \le x \le 1. \end{cases} \qquad (66)$$

From this formula, one can derive the leading behavior of the tails of $\mathcal{P}_G(G,N)$ as

$$\mathcal{P}_G(G,N) \overset{G\to 0}{\approx} \exp\left\{-\frac{\beta}{2}N^2[-\log(4G/N)]\right\} = G^{\beta N^2/2},$$
$$(67)$$

$$\mathcal{P}_G(G,N) \overset{G\to N}{\approx} \exp\left(-\frac{\beta}{2}N^2\{-\log[4(1-G/N)]\}\right) = (N-G)^{\beta N^2/2}$$
$$(68)$$

in agreement with Refs. 38, 39, and 54.

The most interesting feature of Eq. (66) is the appearance of discontinuities in higher-order derivatives at the critical points: more precisely, the third derivative of $\Psi_G(x)$ is discontinuous at $x=1/4$ and $x=3/4$. In fact, Sommers *et al.*[38] found that for finite N_1, N_2 there are several nonanalytical points. Only two of them survive to the leading order $N \to \infty$ and, in our picture, these correspond to a physical phase transition in Laplace space.

In summary, the following exact limit holds:

$$\lim_{N \to \infty} \left[-\frac{2 \log \mathcal{P}_G(Nx,N)}{\beta N^2} \right] = \Psi_G(x), \tag{69}$$

where the rate function $\Psi_G(x)$ is given in Eq. (66).

The free energy difference in Laplace space Eq. (65) for large N has been compared with:

(1) Monte Carlo simulations over the range $p=(-30,30)$, which already for $N=5$ show an excellent agreement (see Fig. 6, left panel). For a given p between -30 and 30, the numerical $J_G(p)$ [and analogously for $J_Q(p)$] is computed as

$$J_G(p) \simeq \frac{\left\langle e^{-pN\Sigma_{i=1}^N x_i} \prod_{j<k} |x_j - x_k|^2 \right\rangle_N}{\left\langle \prod_{j<k} |x_j - x_k|^2 \right\rangle_N}, \tag{70}$$

where the average is taken over N random variables $\{x_i\}$ drawn from a uniform distribution over $(0,1)$.

(2) The *exact* finite N result from Ref. 40 for the Laplace transform of the density in terms of a Hankel determinant [see Eq. (59)]. In Fig. 6 (right panel), we plot our asymptotic result $J_G(p)$, Eq. (65), together with $-\log \mathbf{F}_N(Np;G)/N^2$, where $\mathbf{F}_N(Np;G)$ is the exact finite N result, Eq. (59), for the Laplace transform from Ref. 40 for $-30 \le p \le 30$ and $N = 4, 10$. Already for $N=4$, our $J_G(p)$ reproduces the exact finite N formula with an accuracy of two decimal digits.

V. DISTRIBUTION OF THE SHOT NOISE

The dimensionless shot noise is defined as $P=\Sigma_{i=1}^N T_i(1-T_i)$.[7,8] It is convenient to rewrite it in the form $P=N/4 - \Sigma_{i=1}^N (1/2-T_i)^2 = N/4 - Q$. The probability distributions of P and Q are related by

$$\mathcal{P}_P(P,N) = \mathcal{P}_Q\left(\frac{N}{4} - P, N\right). \tag{71}$$

It is also necessary to make the change of variables in the joint pdf, Eq. (2), $\mu_i = 1/2 - T_i$ so that $-1/2 \le \mu_i \le 1/2$. The joint pdf, Eq. (2), expressed in terms of the new variables μ_i reads

$$P(\mu_1, \ldots, \mu_N) = A_N \prod_{j<k} |\mu_j - \mu_k|^\beta \prod_{i=1}^N \left(\frac{1}{2} - \mu_i\right)^{(\beta/2)-1} \tag{72}$$

and we are interested in the large N decay of the logarithm of $\mathcal{P}_Q(Q,N)$, where $Q=\Sigma_i \mu_i^2$. We have

$$\mathcal{P}_Q(Q,N) = A_N \int_{-1/2}^{1/2} \ldots \int_{-1/2}^{1/2} d\mu_1 \ldots d\mu_N$$

$$\times \exp\left[\frac{\beta}{2} \sum_{j \neq k} \log|\mu_j - \mu_k| \right.$$

$$\left. + \left(\frac{\beta}{2} - 1\right) \sum_{i=1}^N \log\left(\frac{1}{2} - \mu_i\right) \right] \delta\left(\sum_{i=1}^N \mu_i^2 - Q\right). \tag{73}$$

Again, taking the Laplace transform and converting multiple integrals to functional integrals we obtain

$$\int_0^\infty \mathcal{P}_Q(Q,N) e^{-(\beta/2)NpQ} dQ = A_N \int \mathcal{D}[\varrho] e^{-(\beta/2)N^2 S[\varrho_p]}, \tag{74}$$

where for notational simplicity we keep the same symbols ϱ_p and S as before. Of course, the new action S reads

$$S[\varrho_p] = p \int_{-1/2}^{1/2} \varrho_p(\mu)\mu^2 d\mu$$

$$- \int_{-1/2}^{1/2} \int_{-1/2}^{1/2} d\mu d\mu' \varrho_p(\mu)\varrho_p(\mu')\log|\mu - \mu'|$$

$$+ C\left[\int_{-1/2}^{1/2} \varrho_p(\mu)d\mu - 1 \right], \tag{75}$$

where C is the new Lagrange multiplier enforcing the normalization of the charge density to unity.

The stationary point of the action S is determined by

$$\frac{\delta S[\varrho_p]}{\delta \varrho_p} = 0 \tag{76}$$

yielding

$$p\mu^2 + C = 2 \int_{-1/2}^{1/2} d\mu' \varrho_p^\star(\mu')\log|\mu - \mu'|. \tag{77}$$

Taking one more derivative with respect to μ, we get to the following Tricomi equation:

$$p\mu = \mathrm{Pr} \int_{-1/2}^{1/2} \frac{\varrho_p^\star(\mu')}{\mu - \mu'} d\mu'. \tag{78}$$

In terms of the solution $\varrho_p^\star(\mu)$ of Eq. (78), the action in Eq. (75) can be simplified as

$$S[\varrho_p^\star] = \frac{p}{2} \int_{-1/2}^{1/2} \varrho_p^\star(\mu)\mu^2 d\mu - \frac{C}{2}, \tag{79}$$

where the value of the constant C is determined from Eq. (77) by attributing a value to μ within the support of the solution. As in the conductance case, we can write the asymptotic decay of Q as

$$\int_0^\infty \mathcal{P}_Q(Q,N) e^{-(\beta/2)NpQ} dQ \approx \exp\left\{ -\frac{\beta}{2}N^2[S(\varrho_p^\star) - S(\varrho_0^\star)] \right\}$$

$$= \exp\left[-\frac{\beta}{2}N^2 J_Q(p) \right]. \tag{80}$$

Again, in order to solve Eq. (78) we need first to foresee the structure of the allowed support for $\varrho_p^\star(\mu)$. This time, the symmetry constraint $\varrho_p^\star(\mu) = \varrho_p^\star(-\mu)$ reduces the possible behaviors of $\varrho_p^\star(\mu)$ to the following three cases: (I) $\varrho_p^\star(\mu)$ has compact support $[-L,L]$ with $L<1/2$, (II) $\varrho_p^\star(\mu)$ has noncompact support $(-1/2,1/2)$, or (III) the support of $\varrho_p^\star(\mu)$ is the union of two disjoint semicompact intervals $(-1/2,-L] \cup [L,1/2)$ with $L>0$ (see Fig. 8). We analyze the three cases separately.
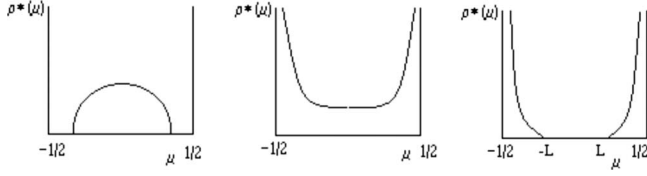
FIG. 8. Density of the auxiliary Q (schematic).

A. Support on $[-L,L]$ with $L < 1/2$

The general solution of Eq. (78) in this case is given by

$$\varrho_p^\star(\mu) = \frac{p}{\pi\sqrt{L^2 - \mu^2}}[c_1 - \mu^2]. \tag{81}$$

The constant c_1 is clearly determined as $c_1 = L^2$ by the condition that $\varrho_p^\star(\pm L) = 0$. Thus, the solution within the bounds $[-L,L]$ with $L < 1/2$ is the semicircle

$$\varrho_p^\star(\mu) = \frac{p}{\pi}\sqrt{L^2 - \mu^2}, \tag{82}$$

where the edge point L is determined by the normalization condition $\int_{-L}^{L}\varrho_p^\star(\mu)d\mu = 1$. This gives

$$L = \sqrt{\frac{2}{p}}, \quad L < 1/2 \Rightarrow p > 8. \tag{83}$$

So, eventually (see Fig. 9)

$$\varrho_p^\star(\mu) = \frac{p}{\pi}\sqrt{\frac{2}{p} - \mu^2}, \quad -\sqrt{\frac{2}{p}} \le \mu \le \sqrt{\frac{2}{p}}, \quad p > 8. \tag{84}$$

Evaluating the action in Eq. (79) [after determining the constant C from Eq. (77) by putting $\mu = 0$ there] we get for $p > 8$

$$S[\varrho_p^\star] = \frac{3}{4} + \frac{1}{2}\log 2 + \frac{1}{2}\log p. \tag{85}$$

From Eq. (80), the value of $J_Q(p) = S[\varrho_p^\star] - S[\varrho_0^\star]$ (still using $S[\varrho_0^\star] = 2\log 2$) for $p \ge 8$ is given by

$$J_Q(p) = \frac{3}{4} + \frac{1}{2}\log\left(\frac{p}{8}\right). \tag{86}$$

Again, the rate function $\Psi_Q(x)$ is given by the inverse Legendre transform of Eq. (86), i.e.,

$$\Psi_Q(x) = \max_p[-xp + J_Q(p)] = \frac{1}{4} - 2\log 2 - \frac{1}{2}\log x \tag{87}$$

valid for $0 \le x \le 1/16$. From Eq. (71), we have the following relation among the rate functions for Q and P:

$$\Psi_P(x) = \Psi_Q\left(\frac{1}{4} - x\right) \tag{88}$$

implying for $\Psi_P(x)$ the following expression:

$$\Psi_P(x) = \frac{1}{4} - 2\log 2 - \frac{1}{2}\log\left(\frac{1}{4} - x\right) \quad \text{for} \quad \frac{3}{16} \le x \le \frac{1}{4}. \tag{89}$$

In Fig. 9 we plot the theoretical density of shifted transmission eigenvalues together with Montecarlo simulations for $N = 6$ and $p = 12$.
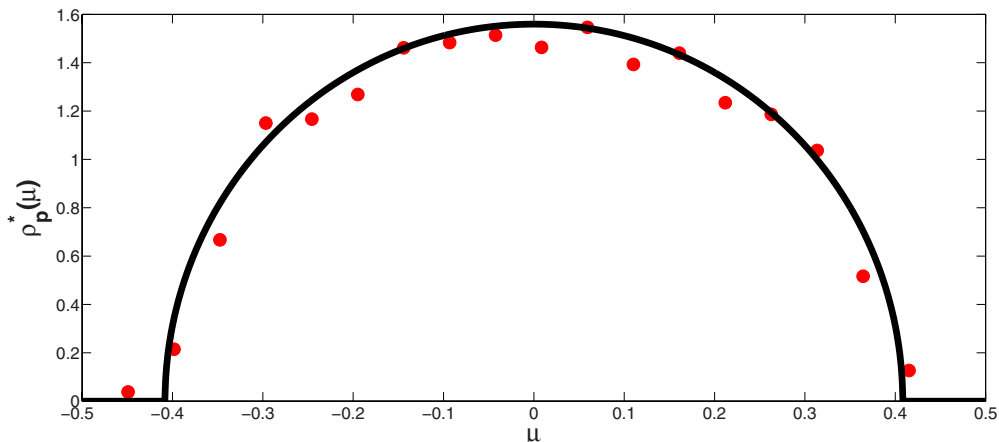
B. Support on $(-1/2, 1/2)$

The general solution of Eq. (78) in this case is given by

$$\varrho_p^\star(\mu) = \frac{p}{\pi\sqrt{1/4 - \mu^2}}[b_1 - \mu^2]. \tag{90}$$

The constant b_1 is determined by the normalization condition $\int_{-1/2}^{1/2}\varrho_p^\star(\mu)d\mu = 1$. This gives $b_1 = 1/p + 1/8$. In turn, the positivity constraint for the density implies $-8 < p < 8$. We then get

$$\varrho_p^\star(\mu) = \frac{p}{\pi\sqrt{1/4 - \mu^2}}\left[\frac{1}{p} + \frac{1}{8} - \mu^2\right],$$

$$\text{for} \quad -\frac{1}{2} < \mu < \frac{1}{2}, \quad -8 < p < 8. \tag{91}$$

Evaluating the action in Eq. (79) gives for $-8 < p < 8$

FIG. 9. (Color online) Density of shifted transmission eigenvalues μ for $N=6$ and $p=12$ (theory vs numerics) for the shot noise case.
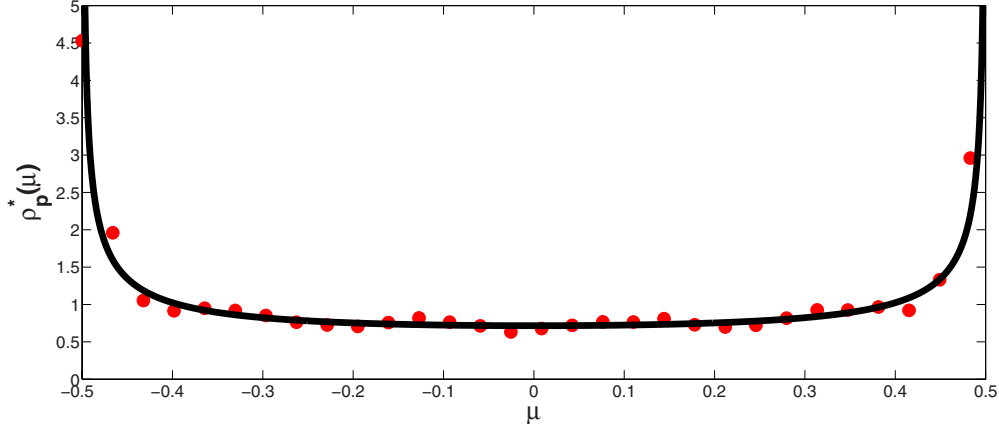
FIG. 10. (Color online) Density of shifted transmission eigenvalues μ for $N=6$ and $p=1$ (theory vs numerics) for the shot noise case.

$$S[\varrho_p^\star] = \frac{p}{8} - \frac{p^2}{256} + 2 \log 2. \tag{92}$$

From Eq. (80), the value of $J_Q(p) = S[\varrho_p^\star] - S[\varrho_0^\star]$ for $-8 \le p \le 8$ is given by

$$J_Q(p) = -\frac{p^2}{256} + \frac{p}{8}. \tag{93}$$

Again, the rate function $\Psi_Q(x)$ is given by the inverse Legendre transform of Eq. (93), i.e.,

$$\Psi_Q(x) = \max_p[-xp + J_Q(p)] = 64\left(x - \frac{1}{8}\right)^2 \tag{94}$$

valid for $1/16 \le x \le 3/16$. From the relation in Eq. (88), we have for $\Psi_P(x)$ the following expression:

$$\Psi_P(x) = 64\left(\frac{1}{8} - x\right)^2 \quad \text{for } \frac{1}{16} \le x \le \frac{3}{16}. \tag{95}$$

In Fig. 10 we plot the theoretical density of shifted transmission eigenvalues together with Montecarlo simulations for $N=6$ and $p=1$.

C. Support on $(-1/2, -L] \cup [L, 1/2)$

For large negative values of p, we envisage a form for the charge density as in Fig. 8 (rightmost panel), i.e., on a disconnected support with two connected and symmetric components. This is because for large negative p, the external potential $p\mu^2$ in Eq. (77) tends to push the charges to the two extreme edges of the box 0 and 1, creating an empty space in the middle. Since we expect to have a disconnected support, we cannot directly use the single support Tricomi solution, Eq. (31). We need to proceed differently.

We start by recasting Eq. (78) in the following form:

$$p\mu = \int_{-1/2}^{-L} \frac{\varrho_p^\star(\mu')}{\mu - \mu'} d\mu' + \Pr \int_L^{1/2} \frac{\varrho_p^\star(\mu')}{\mu - \mu'} d\mu' \quad \mu > 0, \tag{96}$$

$$p\mu = \Pr \int_{-1/2}^{-L} \frac{\varrho_p^\star(\mu')}{\mu - \mu'} d\mu' + \int_L^{1/2} \frac{\varrho_p^\star(\mu')}{\mu - \mu'} d\mu' \quad \mu < 0. \tag{97}$$

In the rhs of Eq. (96) (first integral) we make the change of variables $\mu' \to -\mu'$, getting

$$p\mu = \int_L^{1/2} \frac{\varrho_p^\star(-\mu')}{\mu + \mu'} d\mu' + \Pr \int_L^{1/2} \frac{\varrho_p^\star(\mu')}{\mu - \mu'} d\mu'. \tag{98}$$

Exploiting the symmetry $\varrho_p^\star(\mu) = \varrho_p^\star(-\mu)$, we get

$$p\mu = \Pr \int_L^{1/2} d\mu' \varrho_p^\star(\mu') \left[\frac{1}{\mu + \mu'} + \frac{1}{\mu - \mu'} \right]$$

$$= 2\mu \Pr \int_L^{1/2} d\mu' \frac{\varrho_p^\star(\mu')}{\mu^2 - \mu'^2}. \tag{99}$$

Making a further change of variables $\mu^2 = y$, $\mu'^2 = y'$ we get eventually a Tricomi equation for $\tilde{\varrho}_p(\mu) = \varrho_p^\star(\sqrt{\mu})/\sqrt{\mu}$ as

$$p = \Pr \int_{L^2}^{1/4} dy' \frac{\tilde{\varrho}_p(y')}{y - y'}. \tag{100}$$

Solving Eq. (100) by the standard one support solution, Eq. (31) and converting back to $\varrho_p^\star(\mu)$ we get

$$\varrho_p^\star(\mu) = \frac{|p\mu|(a_2 - \mu^2)}{\pi\sqrt{(1/4 - \mu^2)(\mu^2 - L^2)}}, \tag{101}$$

where a_2 is an arbitrary constant, fixed by the condition $\varrho_p^\star(\pm L) = 0$ (the density is vanishing at the edge points). This gives $a_2 = L^2$. Imposing the normalization condition, we get $L^2 = 1/4 - 2/|p|$. The condition that $L \ge 0$ implies that this solution is valid when $p \le -8$. Thus for $p \le -8$, we then get

$$\varrho_p^\star(\mu) = \frac{|p\mu|\sqrt{\mu^2 - 1/4 + 2/|p|}}{\pi\sqrt{1/4 - \mu^2}}. \tag{102}$$

Note that, when $p \to -8$ from below, the equilibrium solution, Eq. (102), smoothly matches the solution in Eq. (91) in the intermediate regime. The action is readily evaluated from Eq. (79) as
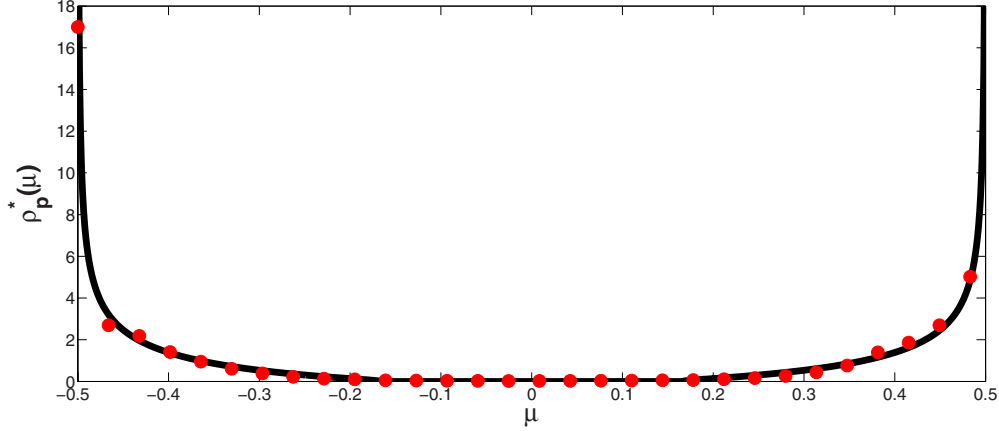
FIG. 11. (Color online) Density of shifted transmission eigenvalues μ for $N=4$ and $p=-9$ (theory vs numerics) for the shot noise case.

$$S[\varrho_p^\star] = p \int_L^{1/2} d\mu \mu^2 \varrho_p^\star(\mu) - 2 \int_L^{1/2} d\mu \varrho_p^\star(\mu) \log \mu$$

$$= \frac{3}{4} + \frac{1}{2}\log(|p|) - \frac{|p|}{4} + \frac{1}{2}\log 2. \qquad (103)$$

The corresponding $J_Q(p)$ is given by

$$J_Q(p) = \frac{3}{4} + \frac{1}{2}\log\left(\frac{|p|}{8}\right) - \frac{|p|}{4} \qquad (104)$$

from which the rate function $\Psi_Q(x)$ can be easily derived

$$\Psi_Q(x) = \max_p[-xp + J_Q(p)] = \frac{1}{4} - 2\log 2 - \frac{1}{2}\log\left(\frac{1}{4} - x\right)$$

$$3/16 \le x \le 1/4. \qquad (105)$$

In Fig. 11 we plot the theoretical density of shifted transmission eigenvalues together with Monte Carlo simulations for $N=4$ and $p=-9$.

D. Final results for the shot-noise case

To summarize, the density of the shifted eigenvalues $\{\mu_i\}$ [solution of the saddle point Eq. (78)] has the following form:

$$\varrho_p^\star(\mu) = \begin{cases} \dfrac{p}{\pi}\sqrt{\dfrac{2}{p} - \mu^2} & -\sqrt{\dfrac{2}{p}} \le \mu \le \sqrt{\dfrac{2}{p}} & p \ge 8 \\[3ex] \dfrac{p}{\pi\sqrt{1/4 - \mu^2}}\left[\dfrac{8+p}{8p} - \mu^2\right] & -1/2 \le \mu \le 1/2 & -8 \le p \le 8 \\[3ex] \dfrac{|p\mu|\sqrt{\mu^2 - 1/4 + 2/|p|}}{\pi\sqrt{1/4 - \mu^2}} & -1/2 \le \mu \le -\sqrt{1/4 - 2/|p|} \vee \sqrt{1/4 - 2/|p|} \le \mu \le 1/2 & p \le -8. \end{cases} \qquad (106)$$

One may easily check that $\varrho_p^\star(\mu)$ is continuous at $p = \pm 8$ but develops two phase transitions characterized by different supports.

The saddle-point action in Eq. (79) is given by

$$S[\varrho_p^\star] = \begin{cases} \dfrac{3}{4} + \dfrac{1}{2}\log 2 + \dfrac{1}{2}\log p & p > 8 \\[2ex] \dfrac{p}{8} - \dfrac{p^2}{256} + 2\log 2 & -8 \le p \le 8 \\[2ex] \dfrac{3}{4} + \dfrac{1}{2}\log(|p|) - \dfrac{|p|}{4} + \dfrac{1}{2}\log 2 & p \le -8, \end{cases} \qquad (107)$$

which is again continuous at $p = \pm 8$.

From Eq. (28), the expression of $J_Q(p) = S[\varrho_p^\star] - S[\varrho_0^\star]$ is

$$J_Q(p) = \begin{cases} \dfrac{3}{4} + \dfrac{1}{2}\log\left(\dfrac{p}{8}\right) & p \ge 8 \\[2ex] \dfrac{-p^2}{256} + \dfrac{p}{8} & -8 \le p \le 8 \\[2ex] \dfrac{3}{4} + \dfrac{1}{2}\log\left(\dfrac{|p|}{8}\right) - \dfrac{|p|}{4} & p \le -8 \end{cases} \qquad (108)$$

from which one can derive (in complete analogy with the conductance case) the rate function for the auxiliary quantity Q

$$\Psi_Q(x) = \begin{cases} \dfrac{1}{4} - 2\log 2 - \dfrac{1}{2}\log x & 0 \le x \le 1/16 \\[2mm] 64\left(x - \dfrac{1}{8}\right)^2 & 1/16 \le x \le 3/16 \\[2mm] \dfrac{1}{4} - 2\log 2 - \dfrac{1}{2}\log\left(\dfrac{1}{4} - x\right) & 3/16 \le x \le 1/4 \end{cases}$$

$$(109)$$

and from the relation $\Psi_P(x) = \Psi_Q(1/4 - x)$ one readily obtains the rate function for the shot noise in Eq. (10).

VI. DISTRIBUTION OF MOMENTS $\mathcal{T}_n$ FOR INTEGER n

In this section, we deal with the more general case of integer moments $\mathcal{T}_n = \Sigma_{i=1}^N T_i^n$, in particular, focusing on the case $n=2$. The conductance is exactly given by $\mathcal{T}_1$ while the shot noise is $\mathcal{T}_1 - \mathcal{T}_2$. While we could use the general method outlined in Sec. III with the choice $a(T) = T^n$, as was done for the conductance case ($n=1$), it turns out that one can obtain the same final results by using a shortcut which combines, in one step, the saddle point evaluation in Eq. (26) and the maximization of the Legendre transform in Eq. (29). Of course, both methods finally yield the same results but this shortcut explicitly avoids any Laplace inversion. Here, we illustrate the shortcut method for the case $a(T) = T^n$ but it can also be used for other linear statistics.

The distribution of the moments $\mathcal{P}_{\mathcal{T}_n}(\mathcal{T}_n = Nt, N)$ is given by

$$\mathcal{P}_{\mathcal{T}_n}(\mathcal{T}_n = Nt, N) = A_N \int_0^1 \dots \int_0^1 dT_1 \dots dT_N$$

$$\times \exp\left[\frac{\beta}{2}\sum_{j \ne k}\log|T_j - T_k|\right.$$

$$\left. + \left(\frac{\beta}{2} - 1\right)\sum_{i=1}^N \log T_i\right]\delta\left(\sum_{i=1}^N T_i^n - Nt\right). \quad (110)$$

The shortcut consists in replacing the delta function by its integral representation: $\delta(x) = \int \frac{dp}{2\pi} e^{px}$ where the integral runs in the complex p plane. The rest is as before, namely, that in the large N limit, one replaces the multiple integral by a functional integral introducing a continuous charge density $\varrho_p(x)$. This gives

$$\mathcal{P}_{\mathcal{T}_n}(\mathcal{T}_n = Nt, N) = A_N \int \frac{dp}{2\pi} \mathcal{D}[\varrho] e^{-(\beta/2)N^2 S[\varrho_p]}, \quad (111)$$

where the action is given by

$$S[\varrho_p] = p\left[\int_0^1 \varrho_p(x)x^n dx - t\right]$$

$$- \int_0^1 \int_0^1 dx dx' \varrho_p(x)\varrho_p(x')\log|x - x'|$$

$$+ C\left[\int_0^1 \varrho_p(x)dx - 1\right], \quad (112)$$

where the rhs of Eq. (111) is now extremized with respect to both $\varrho(x)$ and p. Notice that here we have already performed the inverse Laplace transform of Eq. (23). Hence the two methods are exactly identical.

Extremizing the action gives the following saddle-point equations:

$$px^n + C = 2\int_0^1 dx' \varrho_p^\star(x')\log|x - x'|, \quad (113)$$

$$t = \int_0^1 dx\, x^n \varrho_p^\star(x), \quad (114)$$

which in turn determine p as a function of t.

Multiplying Eq. (113) by $\varrho_p^\star(x)$ and integrating over x, the action at the saddle point can be rewritten in the more compact form

$$S[\varrho_p^\star] = -\frac{1}{2}[pt + C], \quad (115)$$

where, as before, the constant C has to be determined from Eq. (113) by using a suitable value of x which is included in the support of the solution. For large N, Eq. (111) gives

$$\mathcal{P}_{\mathcal{T}_n}(\mathcal{T}_n = Nt, N) \approx \exp\left[-\frac{\beta}{2}N^2\{S[\varrho_p^\star] - S[\varrho_0^\star]\}\right]$$

$$= \exp\left[-\frac{\beta}{2}N^2\Psi_{\mathcal{T}_n}(t)\right], \quad (116)$$

where the rate function is given by

$$\Psi_{\mathcal{T}_n}(t) = S[\varrho_p^\star] - S[\varrho_0^\star] = S[\varrho_p^\star] - 2\log 2 \quad (117)$$

having used again $S[\varrho_0^\star] = 2\log 2$ from Eq. (45).

Upon differentiation of Eq. (113), we obtain the Tricomi equation for $\varrho_p^\star(x)$

$$n\frac{p}{2}x^{n-1} = \mathrm{Pr}\int_0^1 \frac{\varrho_p^\star(x')dx'}{x - x'} \quad (118)$$

to be solved for different supports of $\varrho_p^\star(x)$ as one varies the argument t and consequently the parameter p. As usual, depending on the value of p, we need to first anticipate the "type" of the solution, i.e., the form of its support and then verify it a posteriori, as illustrated below.

A. Large p: support on $(0, L_p]$

Consider first the case when p is very large. Since the external potential in Eq. (113) is of the form $px^n + C$ which is rather steep for large p, we anticipate that the charge fluid will be pushed toward the left hard edge at $x=0$. In this case, the general solution of Eq. (118) with the restriction $n \in \mathbb{N}$ is given by

$$\varrho_p^\star(x) = -\frac{1}{\pi^2\sqrt{x(L_p - x)}}$$
$$\times\left[\frac{1}{2}\mathrm{Pr}\int_0^{L_p}\frac{\sqrt{x'(L_p - x')}np(x')^{n-1}dx'}{x - x'} + C_1\right],$$

(119)

where C_1 is an arbitrary constant. Evaluating the principal value integral yields

$$\varrho_p^\star(x) = -\frac{1}{\pi^2\sqrt{x(L_p - x)}}$$
$$\times\left[-\frac{npL_p^n\sqrt{\pi}\Gamma(n - 1/2)}{4\Gamma(n + 1)}\,{}_2F_1\left(1, -n; 3/2 - n; \frac{x}{L_p}\right) + C_1\right],$$

(120)

where ${}_2F_1(a, b; c; x)$ is a hypergeometric function, defined by the series

$${}_2F_1(a, b; c; x) = 1 + \frac{ab}{c}x + \frac{a(a + 1)b(b + 1)}{c(c + 1)}\frac{x^2}{2!} + \cdots.$$

(121)

Determining the constant C_1 by the requirement that $\varrho_p^\star(L_p) = 0$, we obtain

$$\varrho_p^\star(x) = \frac{1}{\pi(2n - 1)\sqrt{x(L_p - x)}}$$
$$\times[{}_2F_1(1, -n; 3/2 - n; x/L_p) + 2n - 1].$$

(122)

The edge point L_p is finally determined by the normalization requirement $\int_0^{L_p}\varrho_p^\star(x)dx = 1$, yielding after some elementary algebra

$$L_p = \{2\sqrt{\pi}\Gamma(n)/[p\Gamma(n + 1/2)]\}^{1/n}.$$

(123)

Imposing now Eq. (114) as

$$\frac{1}{\pi(2n - 1)}\left\{\int_0^{L_p}\frac{dx\,x^n}{\sqrt{x(L_p - x)}}\right.$$
$$\left.\times[2n - 1 + {}_2F_1(1, -n; 3/2 - n; x/L_p)]\right\} = t$$

(124)

we obtain a very simple relation between p and t

$$p = \frac{1}{tn}.$$

(125)

Armed with Eqs. (125) and (122), we can now evaluate the action in Eq. (115) eliminating p as

$$S[\varrho_p^\star] = \frac{1}{2n} + \log\left(\frac{4}{L_p}\right) = \frac{1}{2n} + 2\log 2$$
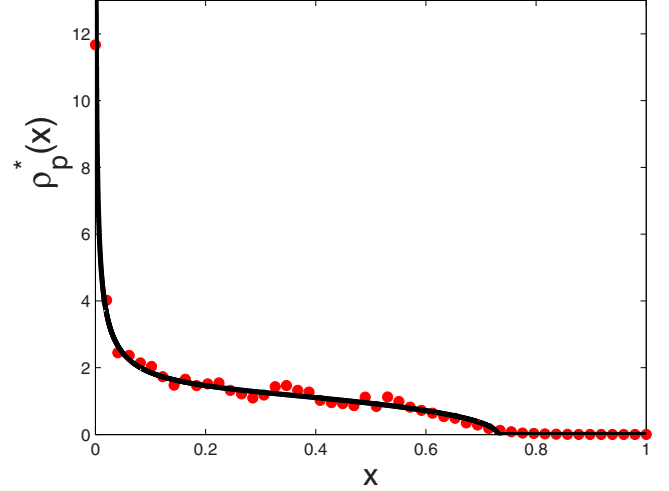$$+ \frac{1}{n}\log\left[\frac{\Gamma(n + 1/2)}{2\sqrt{\pi}\Gamma(n + 1)}t^{-1}\right].$$

(126)

FIG. 12. (Color online) Density of eigenvalues x for $N=5$ and $p=5$ (theory vs numerics) for $n=2$.

Equation (122) is valid as long as $L_p < 1$ [the edge point of the support such that $\varrho_p^\star(L_p) = 0$]. From Eq. (123), putting $L_p = 1$, one thus finds that the solution is valid for $p > p_1^\star$ where

$$p_1^\star = \frac{2\sqrt{\pi}\Gamma(n)}{\Gamma(n + 1/2)}.$$

(127)

Consequently, from Eq. (125), it follows that the solution is valid for $t < t_1^\star$, where

$$t_1^\star = \frac{\Gamma(n + 1/2)}{2\sqrt{\pi}\Gamma(n + 1)}.$$

(128)

As a check, for $n=1$ we have $t_1^\star = 1/4$ from Eq. (128), $L_p = 4/p = 4t$ from Eqs. (123) and (125) and the condition $L_p < 1$ implies $t < t_1^\star = 1/4$ as expected (compare with Sec. IV A). For $n=2$, we have $t_1^\star = 3/16$ and $p_1^\star = 8/3$. For $n=2$, this regime ($t < t_1^\star = 3/16$ and hence $p > p_1^\star = 8/3$) corresponds to the leftmost panel in Fig. 16.

In this region of t, the rate function is easily computed as

$$\Psi_{\mathcal{T}_n}(t) = S[\varrho_p^\star] - 2\log 2$$
$$= \frac{1}{n}\left\{\frac{1}{2} + \log\left[\frac{\Gamma(n + 1/2)}{2\sqrt{\pi}\Gamma(n + 1)}\right] - \log t\right\}.$$

(129)

Combining Eq. (129) with Eq. (116), one obtains as a new result the precise left tail asymptotics for the nth integer moment distribution

$$\mathcal{P}_{\mathcal{T}_n}(\mathcal{T}_n = Nt, N) \approx \exp\left(\frac{\beta N^2}{2n}\log t\right) = t^{\beta N^2/2n}.$$

(130)

In Fig. 12 we plot the theoretical density of eigenvalues for the $n=2$ case together with Montecarlo simulations with $N=5$ and $p=5$.

B. Intermediate p: support on (0,1)

We now look for the solution of

$$n\frac{p}{2}x^{n-1} = \mathrm{Pr}\int_0^1 \frac{\varrho_p^\star(x')}{x-x'}dx' \quad (131)$$

with a nonzero support over the full allowed range [0,1]. Using the general solution in Eq. (31) with the choice $a=0$ and $b=1$ we get

$$\varrho_p^\star(x) = \frac{np\Gamma(n-1/2)}{4\Gamma(n+1)\pi^{3/2}}\left[\frac{{}_2F_1(1,-n;3/2-n;x)-C_n}{\sqrt{x(1-x)}}\right], \quad (132)$$

where C_n is an arbitrary constant to be fixed by $\int_0^1\varrho_p^\star(x)dx = 1$, yielding

$$C_n = -\frac{4\sqrt{\pi}\Gamma(n)}{p\Gamma(n-1/2)} \quad (133)$$

so eventually

$$\varrho_p^\star(x) = \frac{p\Gamma(n-1/2)}{4\Gamma(n)\pi^{3/2}}\left[\frac{{}_2F_1(1,-n;3/2-n;x)+\dfrac{4\sqrt{\pi}\Gamma(n)}{p\Gamma(n-1/2)}}{\sqrt{x(1-x)}}\right]. \quad (134)$$

Next, we need to impose the condition (114)

$$t = \int_0^1 dx\, x^n \varrho_p^\star(x) \quad (135)$$

leading to

$$t = \frac{\Gamma(n+1/2)}{\sqrt{\pi}\Gamma(n+1)}\left[1+\frac{p\Gamma(n-1/2)}{8\sqrt{\pi}\Gamma(n)}(1-2n)\right]. \quad (136)$$

From Eq. (136) we can derive the relation between p and t as

$$p = a_n - b_n t, \quad (137)$$

where

$$a_n = \frac{4\sqrt{\pi}\Gamma(n)}{\Gamma(n+1/2)}, \quad (138)$$

$$b_n = \frac{4\pi\Gamma(n)\Gamma(n+1)}{[\Gamma(n+1/2)]^2}. \quad (139)$$

Inserting Eqs. (137) and (134) into Eq. (115), we obtain, after a few steps of algebra, the action

$$S[\varrho_p^\star] = \frac{b_n}{2}\left[t-\frac{\Gamma(n+1/2)}{\sqrt{\pi}\Gamma(n+1)}\right]^2 + \log 4. \quad (140)$$

Next we need to determine the range of validity of this solution. This is obtained simply by the fact that the density $\varrho_p^\star(x)$ in Eq. (132) must be positive. Let us first rewrite the solution in Eq. (132) as

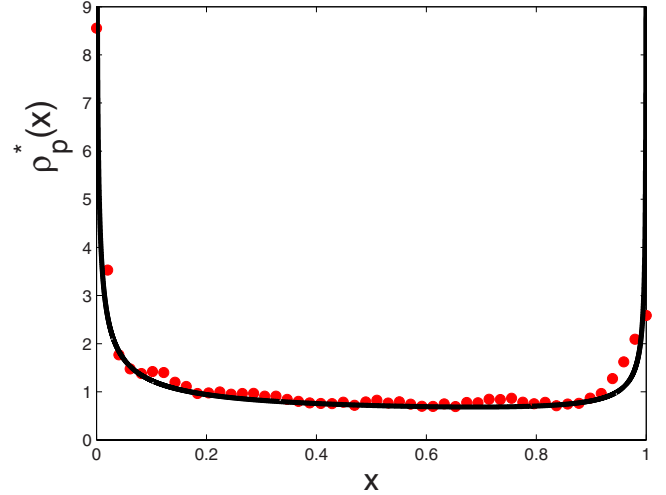$$\varrho_p^\star(x) = \frac{1}{\pi}\frac{A_p(x)}{\sqrt{x(1-x)}}, \quad (141)$$

where

FIG. 13. (Color online) Density of eigenvalues x for $N=6$ and $p=1$ (theory vs numerics) for $n=2$.

$$A_p(x) = 1 + \frac{p\Gamma(n-1/2)}{4\sqrt{\pi}\Gamma(n)}{}_2F_1(1,-n;3/2-n;x). \quad (142)$$

To ensure $\varrho_p^\star(x)\geq 0$, we have to just ensure that $A_p(x)\geq 0$ in Eq. (142). How does $A_p(x)$ vary as a function of x in $x\in[0,1]$? It can be easily seen that this function has a global minimum at some intermediate value $0<x^\star<1$. To ensure its positivity, we then have to ensure that $A_p(x^\star)\geq 0$. This will be true only for a range of values of p, i.e., when $p_2^\star\leq p\leq p_1^\star$ [where $p_1^\star$ is precisely the lower edge of the validity of regime I in the previous section and is given in Eq. (127)]. Consequently, using Eq. (137), this sets a t range $t_1^\star\leq t\leq t_2^\star$ for the validity of this regime II, where $t_1^\star$ is given in Eq. (128). Now, for arbitrary n, $p_2^\star$, and consequently $t_2^\star$ have rather complicated expressions which we do not detail here. But for $n=2$, their expressions are rather simple and we get

$$p_2^\star = -\frac{16}{3}\quad \text{and}\quad t_2^\star = \frac{3}{4}. \quad (143)$$

This then defines regime II with a full support over (0,1), namely, $-16/3\leq p\leq 8/3$ and consequently $3/16\leq t\leq 3/4$, is shown as the second (from the left) region in Fig. 16.

Thus in this regime II where $t_1^\star\leq t_2^\star$, the rate function, for arbitrary n, has a quadratic form

$$\Psi_{\mathcal{T}_n}(t) = S[\varrho_p^\star] - \log 4 = \frac{b_n}{2}\left[t-\frac{\Gamma(n+1/2)}{\sqrt{\pi}\Gamma(n+1)}\right]^2 \quad (144)$$

thus implying Eq. (13)

$$\mathcal{P}_{\mathcal{T}_n}(\mathcal{T}_n,N) \approx \exp\left\{-\frac{\beta}{2}N^2\frac{b_n}{2}\left[\frac{\mathcal{T}_n}{N}-\frac{\Gamma(n+1/2)}{\sqrt{\pi}\Gamma(n+1)}\right]^2\right\}. \quad (145)$$

In Fig. 13 we plot the theoretical density of eigenvalues for the $n=2$ case together with Monte Carlo simulations with $N=6$ and $p=1$. From the Gaussian shape in Eq. (145), the mean and variance of $\mathcal{T}_n$ can be read off very easily
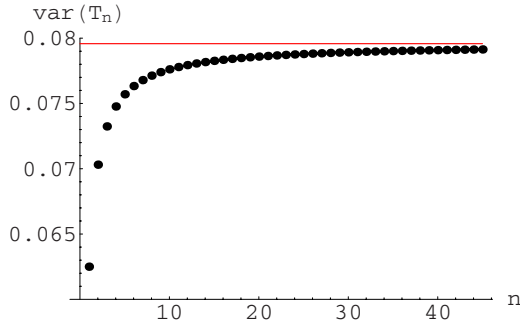
FIG. 14. (Color online) $\mathrm{var}(\mathcal{T}_n)$ as a function of $n \in \mathbb{N}$, Eq. (147), for $\beta=2$. In red the asymptotic value $v^\star = 1/2\pi\beta \approx 0.07957$, Eq. (149).

$$\langle \mathcal{T}_n \rangle = \frac{N\Gamma(n+1/2)}{\sqrt{\pi}\Gamma(n+1)}, \qquad (146)$$

$$\mathrm{var}(\mathcal{T}_n) = \frac{2}{\beta b_n} = \frac{[\Gamma(n+1/2)]^2}{2\beta\pi\Gamma(n)\Gamma(n+1)}. \qquad (147)$$

Novaes[26] recently computed the average of integer moments and obtained the following expression for arbitrary $n \in \mathbb{N}$:

$$\langle \mathcal{T}_n \rangle = N\binom{2n}{n}4^{-n}. \qquad (148)$$

Using elementary properties of Gamma functions, it is easy to show that formulas (146) and (148) do indeed coincide, a fact not completely apparent at first sight.

Conversely, the exact expression for the large N variance, Eq. (147), is new[62] since the general integral in Beenakker's formula[30] does not appear easy to carry out explicitly. Obviously, Eq. (147) agrees with the known result[30] for the conductance $\mathrm{var}(G) = 1/8\beta$ for $n=1$.

From Eq. (147), it is easy to extract the asymptotic value

$$v^\star = \lim_{n \to \infty} \mathrm{var}(\mathcal{T}_n) = \frac{1}{2\beta\pi}, \qquad (149)$$

which is plotted in Fig. 14 for $\beta=2$ together with Eq. (147).

For general n, as one increases the value of t, so far we have seen two regimes: regime I ($0 \le t \le t_1^\star$) with support over $[0, L_p]$ and then regime II ($t_1^\star \le t \le t_2^\star$) with support over the full range $(0,1)$. What happens when t increases beyond $t_2^\star$? For arbitrary n, the analysis becomes rather cumbersome. So from now we restrict ourselves only to the case $n=2$ (which turns out already to be rather nontrivial). But at least for $n=2$ we are able to obtain a full picture and in the two sections below we show that apart from regime I and regime II already discussed above, two further regimes appear as one increases t beyond $t_2^\star$: regime III (for $t_2^\star \le t \le t_3^\star$) where the solution has a disconnected support with two connected components discussed in Sec. VI D and regime IV (for $t_3^\star \le t \le 1$) where the solution again has a single support but on the other side of the box over $[M_p, 1]$. Since the solution in regime IV is simpler (single support), we will first discuss

this case in the next Sec. VI C and finally the more involved case of regime III (with a disconnected support) will be discussed in Sec. VI D.

C. Support on $[M_p, 1](n=2)$: Regime IV

Focusing on the $n=2$ case, we now look for a solution of Eq. (118) with a single support $[M_p, 1]$ where M_p is yet to be determined. Using the general single-support Tricomi solution, Eq. (31), choosing $a=M_p$ and $b=1$, one obtains the following explicit solution:

$$\varrho_p^\star(x) = -\frac{1}{\pi^2\sqrt{(x-M_p)(1-x)}}$$
$$\times \left[p\,\mathrm{Pr}\int_{M_p}^1 \frac{\sqrt{(1-x')(x'-M_p)}}{x-x'}x'dx' + D \right], \qquad (150)$$

where D is an arbitrary constant. Evaluating the principal value integral in Eq. (150) and imposing $\varrho_p^\star(M_p)=0$ we obtain

$$\varrho_p^\star(x) = \frac{-p(2x+M_p-1)}{2\pi}\sqrt{\frac{x-M_p}{1-x}}. \qquad (151)$$

The lower edge M_p is determined by the normalization condition $\int_{M_p}^1 \varrho_p^\star(x)dx=1$, yielding a quadratic equation for M_p: $p(M_p-1)(1+3M_p)=8$ with two roots $M_p = (1 \pm 2\sqrt{1+6/p})/3$. Noting that when $p \to -\infty$, it follows from physical consideration that the charge density must be pushed to its rightmost limit indicating that $M_p \to 1$ as $p \to -\infty$. This condition forces us to choose the correct root as

$$M_p = \frac{1}{3}\left(1 + 2\sqrt{1+\frac{6}{p}}\right). \qquad (152)$$

The condition $0 \le M_p \le 1$ implies for p the condition $p \le p_3^\star = -6$. The relation between p and t is then obtained using Eq. (114), resulting in the condition

$$\frac{15 + 27M_p + 13M_p^2 + 9M_p^3}{16(3M_p+1)} = t, \qquad (153)$$

where M_p is expressed as a function of p in Eq. (152). The solution of Eq. (153) is quite cumbersome to write down explicitly but is, in principle, feasible. Note that when $p \to -6$ from below, $M_p \to 1/3$ from Eq. (152) and consequently from Eq. (153), $t \to t_3^\star = 29/36$ from above. In other words, the solution in Eq. (151) is valid in regime IV defined by

$$p \le p_3^\star = -6; \quad \text{consequently,} \quad t_3^\star = \frac{29}{36} \le t \le 1, \qquad (154)$$

This regime IV is shown in the extreme right part of Fig. 16.

Once p has been determined has a function of t from Eqs. (152) and (153) and substituted into the density, Eq. (151), the action, and the rate function can be computed from Eqs. (115) and (117), by evaluating numerically the corresponding
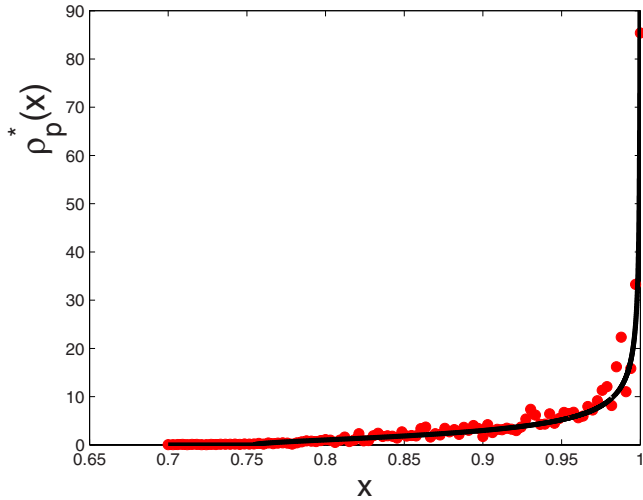
FIG. 15. (Color online) Density of eigenvalues x for $N=4$ and $p=-10$ (theory vs numerics) for $n=2$.

integrals. We omit these details here. In Fig. 15 we plot the theoretical density of eigenvalues for the $n=2$ case together with Monte Carlo simulations with $N=4$ and $p=-10$.

D. Disconnected support ($n=2$): regime III

For $n=2$, it then remains to find the solution of Eq. (118) in the narrow band $t_2^\star=3/4 \leq t \leq t_3^\star=29/36$ or equivalently for $p_3^\star=-6 \leq p \leq p_2^\star=-16/3$ (see Fig. 16). This is the regime III. Let us first try to anticipate what the solution may look like in this regime. For this, let us consider the two regimes, namely, regime II and regime IV, respectively, to the left and right of regime III.

Consider first regime II ($t_1^\star=3/16 \leq t \leq t_2^\star=3/4$). In this regime the solution $\varrho_p^\star(x)$ has a single support over the full
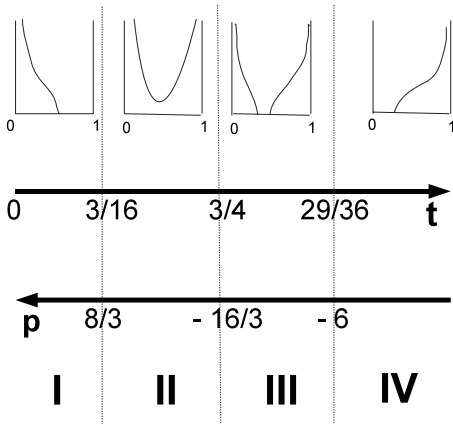

FIG. 16. Schematic table summarizing the relevant phases in the t and p space for the density of $n=2$ moment. As t varies in the allowed range $[0,1]$ and consequently the parameter p in $[-\infty,\infty]$, the fluid density displays four different phases as shown in the top panel. These 4 regimes are separated by three critical points: $t_1^\star=3/16$ (consequently $p_1^\star=8/3$), $t_2^\star=3/4$ ($p_2^\star=-16/3$) and $t_3^\star=29/36$ ($p_3^\star=-6$). Consequently, the rate function $\Psi_{\mathcal{T}_n}(t)$ has four different expressions according to different regions in the $t \in [0,1]$ segment.

range $x \in (0,1)$ given in Eq. (134), which for $n=2$ (using the special value of the hypergeometric function) simply reads, with $p_2^\star=-16/3 \leq p \leq p_1^\star=8/3$

$$\varrho_p^\star(x) = \frac{1}{\pi\sqrt{x(1-x)}}\left[1+\frac{p}{8}(1+4x-8x^2)\right]. \quad (155)$$

Now, when t tends to the maximum allowed value in regime II, namely, $t \to t_2^\star=3/4$ from below or equivalently $p \to p_2^\star=-16/3$ from above, the solution in Eq. (155) tends to

$$\varrho_{-16/3}^\star(x) = \frac{16}{3\pi\sqrt{x(1-x)}}\left[x-\frac{1}{4}\right]^2 \quad (156)$$

with a quadratic minimum at $x=1/4$ where the density vanishes. This is just the edge of regime II. If t increases slightly beyond $t_2^\star=3/4$, this single-support solution is no longer valid. However, it gives the hint that for $t>t_2^\star=3/4$, the charge density must separate into two disjoint components, one on the left side over $[0,l_1]$ and one on the right side over $[l_2,1]$ with an empty stretch $[l_1,l_2]$ separating them. This empty stretch must increase as one increases t beyond $t_2^\star=3/4$ in this regime III. Indeed, as t increases further, the left support $[0,l_1]$ must shrink in size and the right support $[l_2,1]$ must increase in size and finally when t hits the value $t_3^\star=29/36$, l_1 must shrink to 0 and l_2 must approach $M_p=1/3$ and then one arrives in regime IV discussed in the previous section. At exactly $t=t_3^\star=29/36$ or equivalently at $p=p_3^\star=-6$, the solution (border of regime IV) can be read off Eq. (151) with $M_p=1/3$

$$\varrho_{-6}^\star(x) = \frac{6}{\pi\sqrt{1-x}}\left(x-\frac{1}{3}\right)^{3/2}. \quad (157)$$

Thus, the solution in regime III, namely, for $p_3^\star=-6 \leq p \leq p_2^\star=-16/3$ must interpolate between the solutions given in Eqs. (156) and (157) valid, respectively, at the two edges of regime III and have a disconnected support with two connected components over $[0,l_1]$ and $[l_2,1]$. We were able to find this solution explicitly. Its derivation is outlined in the Appendix. The result reads

$$\varrho_p^\star(x) = \frac{-p}{\pi\sqrt{x(1-x)}}\sqrt{(x-l_1)(x-l_2)^3}, \quad (158)$$

which is valid for all $0 \leq x \leq l_1$ and $l_2 \leq x \leq 1$ and the two edges l_1 and l_2 are given by

$$l_1 = \frac{1}{4}\left(1-3\sqrt{1+\frac{16}{3p}}\right), \quad (159)$$

$$l_2 = \frac{1}{4}\left(1+\sqrt{1+\frac{16}{3p}}\right). \quad (160)$$

Note that l_1 and l_2 are real only if $p \leq -16/3$. Furthermore $l_1 \geq 0$ only if $p \geq -6$. Thus this solution is valid over the full range $p_3^\star=-6 \leq p \leq p_2^\star=-16/3$. This then defines regime III. Note also that the solution in Eq. (158) smoothly interpolates between the solutions in Eq. (156) (when $p \to -16/3$) and in Eq. (157) (when $p \to -6$).

The relation between t and p can be obtained substituting Eq. (158) in Eq. (114) and performing the integral. Similarly the action and the rate function can be computed by using the exact density and performing the integrals in Eqs. (115) and (117) by MATHEMATICA, the details of which we omit here. The Monte Carlo simulations in this regimes are much harder to obtain due to large fluctuations in sampling from the leftmost residual band $0 \le x \le l_1$ and a very large N is necessary to achieve a satisfactory picture. Nevertheless, we observed upon increasing N a trend in the equilibrium density which is fully compatible with the analytical disconnected-support solution found above.

E. Final results for the $n=2$ moment case

In Fig. 16 we propose a schematic summary of the different phases of the density of integer moments for the case $n=2$. As a consequence, the rate function will display three (and not just two, as for conductance and shot noise) nonanalytical points corresponding to physical phase transitions in Laplace space. Starting from high p values, the fluid particles are initially confined toward the left hard edge. Then, when p hits the critical value $p=8/3$, the fluid spreads over the entire support $[0,1]$. In the narrow region $-6 \le p \le -16/3$ the density splits over two disjoint (nonsymmetric) components of the support and the leftmost disappears upon hitting the value $p=-6$, leaving the charges leaning against the right hard wall.

VII. CONCLUSIONS

The Coulomb gas analogy, together with recently introduced functional methods, brings about an efficient formalism for the computation of full probability distributions of observables (valid for a large number of electronic channels in the two leads) in the quantum-conductance problem. Generically, the distribution of any linear statistics of the form $A = \sum_{i=1}^{N} a(T_i)$, where the T_i's are transmission eigenvalues of the cavity and $a(x)$ is any smooth function, can be derived within the formalism described in this paper: the problem amounts to finding the equilibrium configuration of an associated 2D charged fluid confined to the segment $[0,1]$ and subject to two competing interactions: the logarithmic repulsion, generated by the Vandermonde term in the jpd, Eq. (2), and a confining potential whose strength is tuned by the Laplace parameter p. Interestingly, this auxiliary Coulomb gas undergoes different phase transitions as the Laplace parameter is varied continuously and this physical picture is mirrored in the appearance of very weak singularities in the rate functions of observables at the critical points. Already the leading N term of the free energy of such a gas (the *spherical* contribution) displays non-Gaussian features in the tails while the central region obeys the Gaussian law, in agreement with the general Politzer's argument;[63] conversely the tails follow a power-law decay and the junctions of the two (or more, as in the case of integer moments) regimes are continuous but nonanalytical points. Note that it is not necessary to develop a $(1/N)$ expansion of the free energy and look for higher genus terms to appreciate deviations from the Gaussian law. From the central Gaussian region, one can easily read off the mean and variance of any linear statistics of interest: this way well known results for, e.g., conductance and shot noise are recovered and new formulas (such as the variance of integer moments and its universal asymptotics) can be derived. Our results are well corroborated by Montecarlo simulations both in the real and Laplace space, as well as by comparison with exact finite N results when available, which convincingly disprove the large-N asymptotic analysis performed in Ref. 40. In summary, the Coulomb gas method (well suited to large N evaluations) reveals a rich thermodynamic behavior for the quantum-conductance problem *already at the leading order level* and we expect that it will enjoy a broad range of applicability.

APPENDIX: EXPLICIT TWO SUPPORT SOLUTION FOR $n=2$ IN REGIME III

We consider the integral Eq. (118) for $n=2$

$$px = \mathrm{Pr} \int_0^1 \frac{\varrho_p^{\star}(x')dx'}{x-x'} \tag{A1}$$

and look for a solution that has a disconnected support with two connected components ($[0,l_1]$ and $[l_2,1]$). This solution is valid in regime III discussed in Sec. VI D. While a general single support solution of the singular integral equation can be found using Tricomi's formula given in Eq. (31) with $g(x)=px$ and discussed in Secs. VI A–VI C, it is much more complicated to obtain an explicit solution with more than one connected component of the support. To find such a solution, we actually use an alternative method originally used by Brezin *et al.*[64] to find a single-support solution of the singular integral equation in the context of counting of planar diagrams. This method consists in making a judicious guess for the solution and then uses the uniqueness properties of analytic functions in a complex plane to prove that the guess is right. Although, for the single-support solution one does not have to use this route since the explicit general solution of Tricomi is available (the authors of[64] were perhaps unaware of the general single-support explicit solution of Tricomi). Nevertheless, this alternative method of Ref. 64 can be fruitfully adapted to find a two support solution (as in our case) in a simpler way (as demonstrated below), where a general solution is somewhat difficult to obtain explicitly.

Let us assume that the solution $\varrho_p^{\star}(x)$ of Eq. (A1) has a disconnected support with two connected components $[0,l_1]$ and $[l_2,1]$ where l_1 and $l_2 \ge l_1$ are yet to be determined. Generalizing the route used for single-support solution in Ref. 64, we first introduce an analytic function [without the principal part in Eq. (A1)]

$$F(x) = \int_0^{l_1} \frac{\varrho_p^{\star}(x')dx'}{x-x'} + \int_{l_2}^1 \frac{\varrho_p^{\star}(x')dx'}{x-x'} \tag{A2}$$

defined everywhere in the complex x plane outside the two real intervals $[0, l_1]$ and $[l_2, 1]$. This new function $F(x)$ has the following properties: (1) it is analytic in the complex x plane outside the two cuts $[0, l_1]$ and $[l_2, 1]$, (2) it behaves as $1/x$ when $|x| \to \infty$ since $\int \varrho_p^\star(x') dx' = 1$ due to normalization, (3) it is real for x real outside the two cuts $[0, l_1]$ and $[l_2, 1]$, and (4) as one approaches to any point x on the two cuts $[0, l_1]$ and $[l_2, 1]$ on the real axis, $F(x \pm i\epsilon) = px \mp i\pi \varrho_p^\star(x)$. This last property follows from Eq. (A1).

From the general properties of analytic functions in the complex plane it follows that there is a unique function $F(x)$ which satisfies all the four properties mentioned above. Thus, if one can make a good guess for $F(x)$ and one verifies that it satisfies all the above properties then this $F(x)$ is unique. Knowing $F(x)$, one can then read off the solution $\varrho_p^\star(x)$ from the fourth property. It then rests to make a good guess for $F(x)$. We try the following ansatz for $F(x)$ valid everywhere outside the two cuts $[0, l_1]$ and $[l_2, 1]$:

$$F(x) = px - \frac{p}{\sqrt{x(x-1)}} \sqrt{(x - l_1)(x - l_2)^3}. \qquad (A3)$$

This ansatz clearly satisfies the first property. Now, expanding $F(x)$ for large $|x|$ we get

$$F(x) \to (-1 + l_1 + 3l_2)p + \frac{p}{8}(-3 + 2l_1 + l_1^2$$
$$+ 6l_2 - 6l_1 l_2 - 3l_2^2)\frac{1}{x} + O(x^{-2}). \qquad (A4)$$

Since the second property dictates that $F(x) \to 1/x$, it follows that we must have

$$l_1 + 3l_2 = 1, \qquad (A5)$$

$$(-3 + 2l_1 + l_1^2 + 6l_2 - 6l_1 l_2 - 3l_2^2) = 8. \qquad (A6)$$

Eliminating l_2 in Eq. (A6) using Eq. (A5) gives a quadratic equation for l_1, $2l_1^2 - l_1 - 1 = 6/p$ with two solutions: $l_1 = (1 \pm 3\sqrt{16/p})/4$. The correct root is chosen by the fact that when $p \to -6$, $l_1 \to 0$ as follows from the solution in Eq. (157). This then uniquely fixes l_1 and l_2 given, respectively, in Eqs. (159) and (160).

The ansatz $F(x)$, with the choices l_1 and l_2 as in Eqs. (159) and (160) then satisfies the second property. It is easy to check that $F(x)$ satisfies the third property as well. From the fourth property one then reads off the unique solution as given in Eq. (158). This two support solution is clearly valid only in the regime III, namely, for $p_3^\star = -6 \leq p \leq p_2^\star = -16/3$ and it smoothly matches with the solutions of regime II and regime IV, respectively, as $p \to -16/3$ and $p \to -6$.

[1] C. W. J. Beenakker, Rev. Mod. Phys. **69**, 731 (1997).

[2] A. M. Chang, H. U. Baranger, L. N. Pfeiffer, and K. W. West, Phys. Rev. Lett. **73**, 2111 (1994).

[3] C. M. Marcus, A. J. Rimberg, R. M. Westervelt, P. F. Hopkins, and A. C. Gossard, Phys. Rev. Lett. **69**, 506 (1992).

[4] S. Oberholzer, E. V. Sukhorukov, C. Strunk, C. Schönenberger, T. Heinzel, and M. Holland, Phys. Rev. Lett. **86**, 2114 (2001).

[5] R. Landauer, IBM J. Res. Dev. **1**, 223 (1957); Philos. Mag. **21**, 863 (1970); D. S. Fisher and P. A. Lee, Phys. Rev. B **23**, 6851 (1981).

[6] M. Büttiker, Phys. Rev. Lett. **57**, 1761 (1986).

[7] Ya. M. Blanter and M. Büttiker, Phys. Rep. **336**, 1 (2000).

[8] G. B. Lesovik, JETP Lett. **49**, 592 (1989).

[9] K. Richter and M. Sieber, Phys. Rev. Lett. **89**, 206801 (2002).

[10] P. Braun, S. Heusler, S. Müller, and F. Haake, J. Phys. A **39**, L159 (2006).

[11] G. Berkolaiko, J. M. Harrison, and M. Novaes, J. Phys. A: Math. Theor. **41**, 365102 (2008).

[12] H. Schanz, M. Puhlmann, and T. Geisel, Phys. Rev. Lett. **91**, 134101 (2003).

[13] R. S. Whitney and Ph. Jacquod, Phys. Rev. Lett. **96**, 206804 (2006).

[14] K. A. Muttalib, J. L. Pichard, and A. D. Stone, Phys. Rev. Lett. **59**, 2475 (1987).

[15] A. D. Stone, P. A. Mello, K. A. Muttalib, and J. L. Pichard, in *Mesoscopic Phenomena in Solids*, edited by B. L. Altshuler, P. A. Lee, and R. A. Webb (North-Holland, Amsterdam, 1991).

[16] P. A. Mello, P. Pereyra, and N. Kumar, Ann. Phys. (N.Y.) **181**, 290 (1988).

[17] B. L. Altshuler and B. I. Shklovskii, Zh. Eksp. Teor. Fiz. **91**, 220 (1986); [Sov. Phys. JETP **64**, 127 (1986)].

[18] M. L. Mehta, *Random Matrices*, 3rd ed. (Elsevier, Academic, New York, 2004).

[19] F. J. Dyson, J. Math. Phys. **3**, 140 (1962); **3**, 157 (1962); **3**, 166 (1962).

[20] P. J. Forrester, J. Phys. A **39**, 6861 (2006).

[21] J. E. F. Araújo and A. M. S. Macêdo, Phys. Rev. B **58**, R13379 (1998).

[22] A is a linear statistics in that it does not contain products of different eigenvalues. The function $a(x)$ may well depend nonlinearly on x.

[23] Ya. M. Blanter, H. Schomerus, and C. W. J. Beenakker, Physica E **11**, 1 (2001); Yu. V. Nazarov and D. A. Bagrets, Phys. Rev. Lett. **88**, 196801 (2002); S. Pilgram, A. N. Jordan, E. V. Sukhorukov and M. Büttiker, *ibid.* **90**, 206801 (2003); E. V. Sukhorukov and O. M. Bulashenko, *ibid.* **94**, 116803 (2005); S. Pilgram, P. Samuelsson, H. Förster and M. Büttiker, *ibid.* **97**, 066801 (2006) O. M. Bulashenko, J. Stat. Mech. **2005**, P08013; L. S. Levitov and G. B. Lesovik, JETP Lett. **58**, 230 (1993); H. Lee, L. S. Levitov, and A. Yu. Yakovets, Phys. Rev. B **51**, 4079 (1995).

[24] W. Lu, Z. Ji, L. Pfeiffer, K. W. West, and A. J. Rimberg, Nature (London) **423**, 422 (2003); J. Bylander, T. Duty and P. Delsing, *ibid.* **434**, 361 (2005); T. Fujisawa, T. Hayashi, Y. Hirayama, H. D. Cheong, and Y. H. Jeong, Appl. Phys. Lett. **84**, 2343 (2004); R. Schleser, E. Ruh, T. Ihn, K. Ensslin, D. C. Driscoll, and A. C. Gossard, *ibid.* **85**, 2005 (2004); E. V. Sukhorukov, A. N. Jordan, S. Gustavsson, R. Leturcq, T. Ihn, and K. Ensslin, Nat. Phys. **3**, 243 (2007).

[25] P. W. Brouwer and C. W. J. Beenakker, J. Math. Phys. **37**, 4904

(1996).

[26] M. Novaes, Phys. Rev. B **75**, 073304 (2007); **78**, 035337 (2008).

[27] D. V. Savin and H.-J. Sommers, Phys. Rev. B **73**, 081307(R) (2006).

[28] D. V. Savin, H.-J. Sommers, and W. Wieczorek, Phys. Rev. B **77**, 125332 (2008).

[29] P. Vivo and E. Vivo, J. Phys. A: Math. Theor. **41**, 122004 (2008).

[30] C. W. J. Beenakker, Phys. Rev. Lett. **70**, 1155 (1993).

[31] E. N. Bulgakov, V. A. Gopar, P. A. Mello, and I. Rotter, Phys. Rev. B **73**, 155302 (2006).

[32] H. U. Baranger and P. A. Mello, Phys. Rev. Lett. **73**, 142 (1994).

[33] R. A. Jalabert, J.-L. Pichard, and C. W. J. Beenakker, Europhys. Lett. **27**, 255 (1994).

[34] A. García-Martín and J. J. Sáenz, Phys. Rev. Lett. **87**, 116603 (2001).

[35] K. A. Muttalib and P. Wölfle, Phys. Rev. Lett. **83**, 3013 (1999); A. Cresti, R. Farchioni, and G. Grosso, Eur. Phys. J. B **46**, 133 (2005); K. A. Muttalib, P. Wölfle, A. García-Martín, and V. A. Gopar, Europhys. Lett. **61**, 95 (2003); L. S. Froufe-Pérez, P. García-Mochales, P. A. Serena, P. A. Mello, and J. J. Sáenz, Phys. Rev. Lett. **89**, 246403 (2002); V. A. Gopar, K. A. Muttalib, and P. Wölfle, Phys. Rev. B **66**, 174204 (2002).

[36] K. A. Muttalib, P. Markoš, and P. Wölfle, Phys. Rev. B **72**, 125317 (2005); P. Markoš, *ibid.* **65**, 104207 (2002).

[37] M. H. Pedersen, S. A. van Langen, and M. Büttiker, Phys. Rev. B **57**, 1838 (1998).

[38] H.-J. Sommers, W. Wieczorek, and D. V. Savin, Acta Phys. Pol. A **112**, 691 (2007).

[39] B. A. Khoruzhenko, D. V. Savin, and H.-J. Sommers, Phys. Rev. B **80**, 125301 (2009).

[40] V. Al Osipov and E. Kanzieper, Phys. Rev. Lett. **101**, 176804 (2008).

[41] V. Al Osipov and E. Kanzieper, J. Phys. A: Math. Theor. **42**, 475101 (2009).

[42] P. Vivo, S. N. Majumdar, and O. Bohigas, Phys. Rev. Lett. **101**, 216809 (2008).

[43] S. Hemmady, J. Hart, X. Zheng, T. M. Antonsen, E. Ott, and S. M. Anlage, Phys. Rev. B **74**, 195326 (2006).

[44] Hereafter we will use the concise notation $\mathcal{P}(A,N) \approx \exp[-\frac{\beta}{2}N^2\Psi_A(A/N)]$ to mean exactly Eq. (7).

[45] D. S. Dean and S. N. Majumdar, Phys. Rev. Lett. **97**, 160201 (2006); Phys. Rev. E **77**, 041108 (2008).

[46] A. J. Bray and D. S. Dean, Phys. Rev. Lett. **98**, 150201 (2007).

[47] Y. V. Fyodorov, H.-J. Sommers, and I. Williams, JETP Lett. **85**, 261 (2007).

[48] Y. V. Fyodorov and I. Williams, J. Stat. Phys. **129**, 1081 (2007).

[49] C. Nadal and S. N. Majumdar, Phys. Rev. E **79**, 061117 (2009).

[50] S. N. Majumdar and M. Vergassola, Phys. Rev. Lett. **102**, 060601 (2009).

[51] C. Nadal, S. N. Majumdar and M. Vergassola, arXiv:0911.2844 (unpublished).

[52] S. N. Majumdar, C. Nadal, A. Scardicchio, and P. Vivo, Phys. Rev. Lett. **103**, 220603 (2009).

[53] P. Vivo, S. N. Majumdar, and O. Bohigas, J. Phys. A: Math. Theor. **40**, 4317 (2007).

[54] P. A. Mello and H. U. Baranger, Waves Random Media **9**, 105 (1999).

[55] H. Touchette, Phys. Rep. **478**, 1 (2009).

[56] Note that such a nice feature is a direct consequence of having employed the *correct* speed $\alpha=1$, i.e., of having scaled the Laplace parameter z with N in the correct way.

[57] F. G. Tricomi, *Integral Equations* (Interscience, London, 1957).

[58] P. Facchi, U. Marzolino, G. Parisi, S. Pascazio, and A. Scardicchio, Phys. Rev. Lett. **101**, 050502 (2008).

[59] P. Kazakopoulos, P. Mertikopoulos, A. L. Moustakas, and G. Caire, arXiv:0907.5024 (unpublished).

[60] W. Krauth, *Statistical Mechanics: Algorithms and Computation* (Oxford University Press, Oxford, 2006).

[61] We are grateful to Céline Nadal for performing this simulation for us.

[62] Novaes has recently computed the variance for any finite number of open channels N_1 and N_2 (Ref. 26): however, extracting the asymptotics from his formula does not appear to be easy.

[63] H. D. Politzer, Phys. Rev. B **40**, 11917 (1989).

[64] E. Brézin, C. Itzykson, G. Parisi, and J. B. Zuber, Commun. Math. Phys. **59**, 35 (1978).